

# We are IntechOpen, the world's leading publisher of Open Access books Built by scientists, for scientists

6,900

Open access books available

186,000

International authors and editors

200M

Downloads

Our authors are among the

154

Countries delivered to

TOP 1%

most cited scientists

12.2%

Contributors from top 500 universities



WEB OF SCIENCE™

Selection of our books indexed in the Book Citation Index  
in Web of Science™ Core Collection (BKCI)

Interested in publishing with us?  
Contact [book.department@intechopen.com](mailto:book.department@intechopen.com)

Numbers displayed above are based on latest data collected.  
For more information visit [www.intechopen.com](http://www.intechopen.com)



# Dye Sensitized Solar Cells - Working Principles, Challenges and Opportunities

Khalil Ebrahim Jasim

Department of Physics, University of Bahrain  
Kingdom of Bahrain

## 1. Introduction

Even before the industrial revolutions human life quality is greatly affected by the availability of energy. The escalated and savage consumption of conventional sources of energy are leading to forecasted energy and environmental crises. Renewable energy sources such as solar energy are considered as a feasible alternative because *“More energy from sunlight strikes Earth in 1 hour than all of the energy consumed by humans in an entire year.”* (Lewis, 2007). Facilitating means to harvest a fraction of the solar energy reaching the Earth may solve many problems associated with both the energy and global environment (Nansen, 1995). Therefore, intensive research activities have resulted in attention-grabbing to the different classes of organic and inorganic based solar cells. A major study by IntertechPira stated that *“The global Photovoltaic (PV) market, after experiencing a slow period, is expected to double within the next five years, reaching US\$ 48 billion. Wafer-based silicon will continue as the dominant technology, but amorphous thin-film and Cadmium Telluride (CdTe) technologies will gain ground, and are expected to account for a combined 22% of the market by 2014”* (www.intertechpira.com).

A solar cell is a photonic device that converts photons with specific wavelengths to electricity. After Alexandre Edmond Becquerel (French physicist) discovered the photoelectrochemical (photovoltaic) effect in 1839 (Becquerel, 1839) while he was investigating the effect of light on metal electrodes immersed in electrolyte, research in this area continued and technology developed to produce many types and structures of the materials presently used in photovoltaic (PV) technology. First and second generations photovoltaic cells are mainly constructed from semiconductors including crystalline silicon, III-V compounds, cadmium telluride, and copper indium selenide/sulfide (Hara & Arakawa, 2003; Hoffert, 1998; Zhao et al., 1999). Low cost solar cells have been the subject of intensive research work for the last three decades. Amorphous semiconductors were announced as one of the most promising materials for low cost energy production. However, dye sensitized solar cells DSSCs emerged as a new class of low cost energy conversion devices with simple manufacturing procedures. General comparison between semiconductor based solar cells and dye sensitized solar cells is presented in Table 1.

Incorporation of dye molecules in some wide bandgap semiconductor electrodes was a key factor in developing photoelectrochemical solar cells. Michael Gratzel and coworkers at the Ecole Polytechnique Federale de Lausanne (Gratzel, 2003; Nazerruddin et al., 1993; O' Regan & Gratzel, 1991) succeeded for the first time to produce what is known as *“Gratzel Cell”* or

the dye sensitized solar cell (DSSC) to imitate photosynthesis -the natural processes plants convert sunlight into energy- by sensitizing a nanocrystalline TiO<sub>2</sub> film using novel Ru bipyridyl complex. In dye sensitized solar cell DSSC charge separation is accomplished by kinetic competition like in photosynthesis leading to photovoltaic action. It has been shown that DSSC are promising class of low cost and moderate efficiency solar cell (see Table 2 and Figure 1) based on organic materials (Gratzel, 2003; Hara & Arakawa, 2003).

	Semiconductor solar cells	DSSC
Transparency	Opaque	Transparent
Pro-Environment (Material & Process)	Normal	Great
Power Generation Cost	High	Low
Power Generation Efficiency	High	Normal
Color	Limited	Various

Table 1. Comparison between semiconductor based solar cell and the dye sensitized solar cell DSSC.

In fact, in semiconductor p-n junction solar cell charge separation is taken care by the junction built in electric field, while in dye sensitized solar cell charge separation is by kinetic competition as in photosynthesis (Späth et al., 2003). The organic dye monolayer in the photoelectrochemical or dye sensitized solar cell replaces light absorbing pigments (chlorophylls), the wide bandgap nanostructured semiconductor layer replaces oxidized dihydro-nicotinamide-adenine-dinucleotide phosphate (NADPH), and carbon dioxide acts as the electron acceptor. Moreover, the electrolyte replaces the water while oxygen as the electron donor and oxidation product, respectively (Lagref. et al., 2008; Smestad & Gratzel, 1998). The overall cell efficiency of dye sensitized solar cell is found to be proportional to the electron injection efficiency in the wide bandgap nanostructured semiconductors. This finding has encouraged researchers over the past decade. ZnO<sub>2</sub> nanowires, for example, have been developed to replace both porous and TiO<sub>2</sub> nanoparticle based solar cells (Law et al., 2005). Also, metal complex and novel man made sensitizers have been proposed (Hasselmann & Meyer, 1999; Isalm et al., 2000; Yang et al., 2000). However, processing and synthesization of these sensitizers are complicated and costly processes (Amao & Komori 2004; Garcia et al., 2003; Hao et al., 2006; Kumara et al., 2006; Polo & Iha, 2006; Smestad, 1998; Yanagida et al., 2004). Development or extraction of photosensitizers with absorption range extended to the near IR is greatly desired. In our approach, the use of natural dye extracts, we found that our environment provides natural, non toxic and low cost dye sources with high absorbance level of UV, visible and near IR. Examples of such dye sources are Bahraini Henna (*Lawsonia inermis* L.) and Bahraini raspberries (*Rubus* spp.). In this work we provide further details about the first reported operation of Henna (*Lawsonia inermis* L.) as a natural dye sensitizer of TiO<sub>2</sub> nanostructured solar cell (Jasim & Hassan, 2009; Jasim et al. in press 2011). We have experienced the usefulness of commercialized dye sensitized solar cell kits such as the one provided by Dyesol™ to “illustrates how interdisciplinary science can be taught at lower division university and upper division high school levels for an understanding of renewable energy as well as basic science concepts.” (Smestad, 1998; Smestad & Gratzel 1998) Furthermore, it aids proper training and awareness about the role of nanotechnology in modern civilization.

Classification	$\eta$ [%]	Area <sup>[a]</sup> [cm <sup>2</sup> ]	$V_{oc}$ [V]	$J_{sc}$ [mA · cm <sup>-2</sup> ]	$FF$ [-]	Test center <sup>[b]</sup> (and date)	Producer
<b>Silicon</b>							
Si (crystalline)	24.7±0.5	4.00 (da)	0.706	42.2	0.83	Sandia (3/99)	UNSW PERL
Si (multicrystalline)	19.8±0.5	1.09 (ap)	0.654	38.1	0.80	Sandia (2/98)	UNSW/Eurosolare
Si (thin-film transfer)	16.6±0.4	4.02 (ap)	0.645	32.8	0.78	FhG-ISE (7/01)	U. Stuttgart
<b>III-V cells</b>							
GaAs (crystalline)	25.1±0.8	3.91 (t)	1.022	28.2	0.87	NREL (3/90)	Kopin
GaAs (thin film)	23.3±0.7	4.00 (ap)	1.011	27.6	0.84	NREL (4/90)	Kopin
GaAs (multicrystalline)	18.2±0.5	4.01 (t)	0.994	23.0	0.80	NREL (11/95)	RTI
InP (crystalline)	21.9±0.7	4.02 (t)	0.878	29.3	0.85	NREL (4/90)	Spire
<b>Polycrystalline thin film</b>							
CuInGaSe <sub>2</sub> (CIGS)	18.4±0.5	1.04 (t)	0.669	35.7	0.77	NREL (2/01)	NREL
CdTe	16.5±0.5	1.13 (ap)	0.845	26.7	0.76	NREL (9/01)	NREL
<b>Amorphous/microcrystalline Si</b>							
Si (nanocrystalline)	10.1±0.2	1.20 (ap)	0.539	24.4	0.77	JQA (12/97)	Kaneka
<b>Photoelectrochemical cells</b>							
Nanocrystalline dye	11.0±0.5	0.25 (ap)	0.795	19.4	0.71	FhG-ISE (12/96)	EPFL, LPI
Nanocrystalline dye (submodule)	4.7±0.2	141.4 (ap)	0.795	11.3	0.59	FhG-ISE (2/98)	INAP
<b>Multijunction cells</b>							
GaInP/GaAs	30.3	4.0 (t)	2.488	14.22	0.86	JQA (4/96)	Japan Energy
GaInP/GaAs/Ge	28.7±1.4	29.93 (t)	2.571	12.95	0.86	NREL (9/99)	Spectrolab
GaAs/CIS (thin film)	25.8±1.3	4.00 (t)	–	–	–	NREL (11/89)	Kopin/Boing
a-Si/CIGS (thin film)	14.6±0.7	2.40 (ap)	–	–	–	NREL (6/88)	ARCO

Table 2. Confirmed terrestrial cell efficiencies measured under the global AM 1.5 spectrum (1000 W · m<sup>-2</sup>) at 25 °C. [a] (ap)=aperture area; (t)=total area; (da)=designated irradiance area. [b] FhG-ISE=Fraunhofer-Institute for Solar Energy system; JQA = Japan Quality Assurance (From Green & Emery, 2002).

In this chapter, we overview some aspects of the historical background, present, and anticipated future of dye sensitized solar cells. Operation principle of the dye sensitized solar cell is explained. Some schemes used in preparation and assembly of dye sensitized solar cell are presented with few recommendations that might lead to better performance and stability of the fabricated cell. The structural, optical, electrical, and photovoltaic performance stability of DSSC are discussed. The performance of nanocrystalline solar cell samples can be appreciably improved by optimizing the preparation technique, the class of the nanostructured materials, types of electrolyte, and high transparent conductive electrodes. Challenges associated with materials choice, nanostructured electrodes and device layers structure design are detailed. Recent trends in the development of

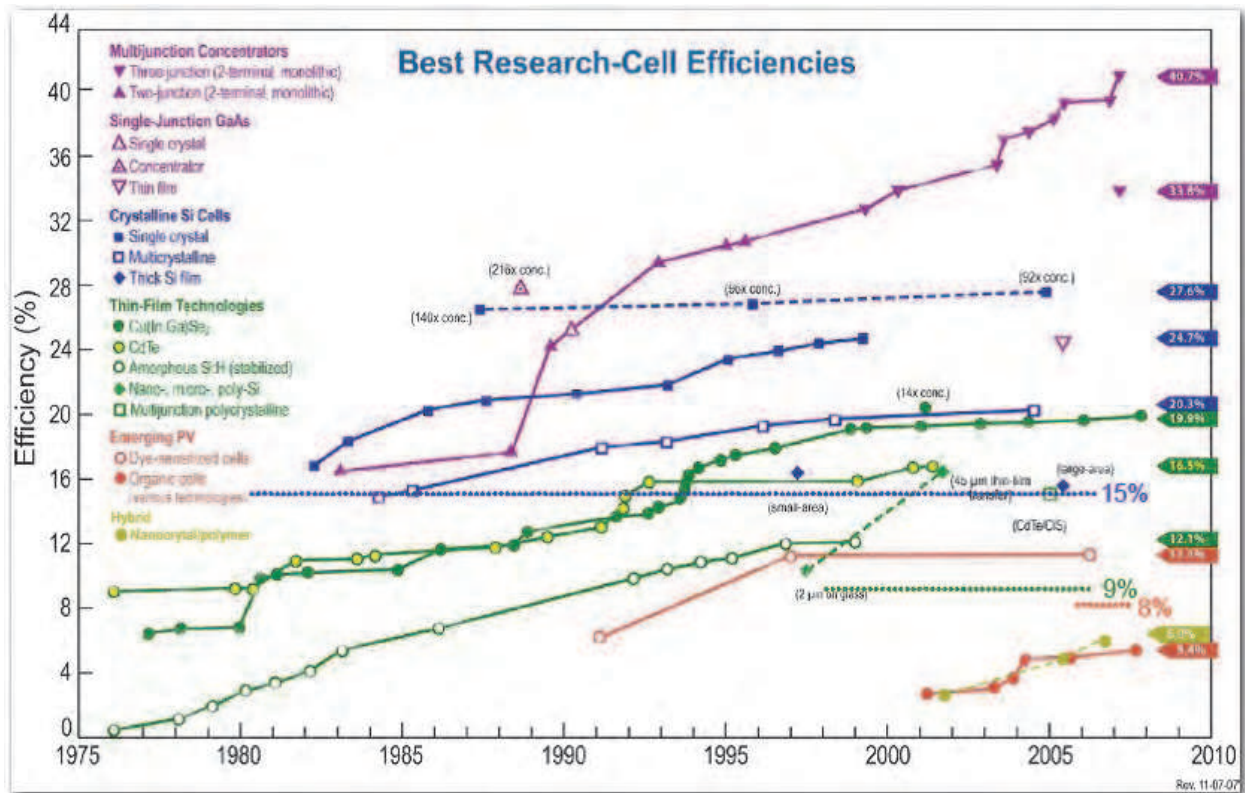


Fig. 1. Reported best research cell efficiencies (Source: National Renewable Laboratory, 2007). The Overall peak power production of dye sensitized solar cell represents a conversion efficiency of about 11%.

nano-crystalline materials for DSSCs technology are introduced. Manufacturability and different approaches suggested for commercialization of DSSC for various applications are outlined. We believe that the availability of efficient natural dye sensitizers, flexible and ink-printable conductive electrodes, and solid state electrolyte may enhance the development of a long term stable DSSCs and hence the feasibility of outdoor applications of both the dye sensitized solar cells and modules.

## 2. Structure of dye sensitized solar cell

The main parts of single junction dye sensitized solar cell are illustrated schematically in Figure 2. The cell is composed of four elements, namely, the transparent conducting and counter conducting electrodes, the nanostructured wide bandgap semiconducting layer, the dye molecules (sensitizer), and the electrolyte. The transparent conducting electrode and counter-electrode are coated with a thin conductive and transparent film such as fluorine-doped tin dioxide ( $\text{SnO}_2$ ).

### 2.1 Transparent substrate for both the conducting electrode and counter electrode

Clear glass substrates are commonly used as substrate because of their relative low cost, availability and high optical transparency in the visible and near infrared regions of the electromagnetic spectrum. Conductive coating (film) in the form of thin transparent conductive oxide (TCO) is deposited on one side of the substrate. The conductive film ensures a very low electric resistance per square. Typical value of such resistance is 10-20  $\Omega$

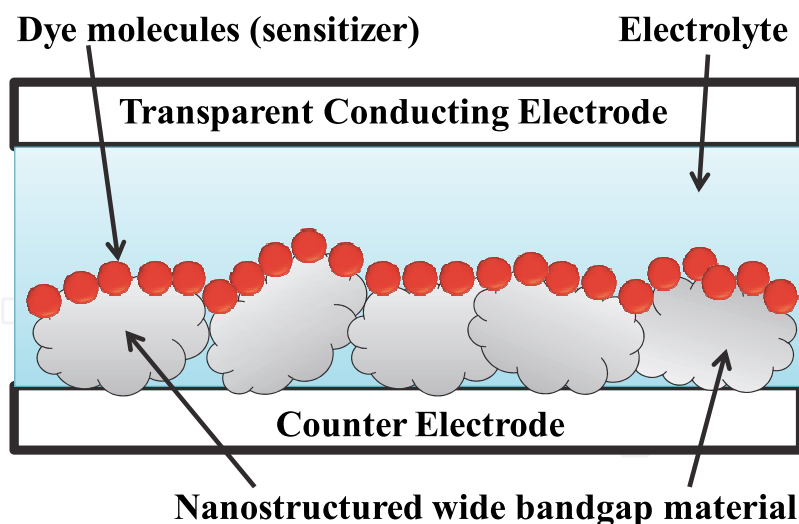


Fig. 2. Schematic of the structure of the dye sensitized solar cell.

per square at room temperature. The nanostructured wide bandgap oxide semiconductor (electron acceptor) is applied, printed or grown on the conductive side. Before assembling the cell the counter electrode must be coated with a catalyzing layer such as graphite layer to facilitates electron donation mechanism to the electrolyte (electron donor) as well be discussed later.

One must bear in mind that the transparency levels of the transparent conducting electrode after being coated with the conductive film is not 100% over the entire visible and near infrared (NIR) part of the solar spectrum. In fact, the deposition of nanostructured material reduces transparency of the electrode. Figure 3 shows a typical transmittance measurement (using dual beam spectrophotometer) of conductive glass electrode before and after being coated with nanostructured  $\text{TiO}_2$  layer.

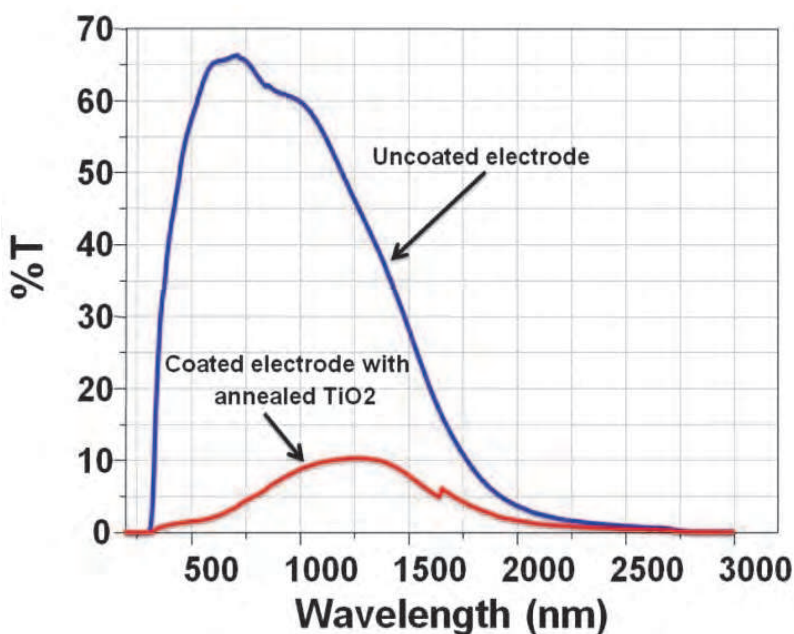


Fig. 3. Transmittance of conductive glass electrode before and after being coated with nanostructured  $\text{TiO}_2$  layer.

## 2.2 Nanostructured photoelectrode

In the old generations of photoelectrochemical solar cells (PSC) photoelectrodes were made from bulky semiconductor materials such as Si, GaAs or CdS. However, these kinds of photoelectrodes when exposed to light they undergo photocorrosion that results in poor stability of the photoelectrochemical cell. The use of sensitized wide bandgap semiconductors such as  $\text{TiO}_2$ , or  $\text{ZnO}_2$  resulted in high chemical stability of the cell due to their resistance to photocorrosion. The problem with bulky single or poly-crystalline wide bandgap is the low light to current conversion efficiency mainly due to inadequate adsorption of sensitizer because of limited surface area of the electrode. One approach to enhance light-harvesting efficiency (LHE) and hence the light to current conversion efficiency is to increase surface area (the roughness factor) of the sensitized photoelectrode.

Due to the remarkable changes in mechanical, electrical, magnetic, optical and chemical properties of nanostructured materials compared to its phase in bulk structures, it received considerable attention (Gleiter, 1989). Moreover, because the area occupied by one dye molecule is much larger than its optical cross section for light capture, the absorption of light by a monolayer of dye is insubstantial. It has been confirmed that high photovoltaic efficiency cannot be achieved with the use of a flat layer of semiconductor or wide bandgap semiconductor oxide surface but rather by use of nanostructured layer of very high roughness factor (surface area). Therefore, Gratzel and his coworkers replaced the bulky layer of titanium dioxide ( $\text{TiO}_2$ ) with nonporous  $\text{TiO}_2$  layer as a photoelectrode. Also, they have developed efficient photosensitizers (new Ru complex, see for example Figure 16) that are capable of absorbing wide range of visible and near infrared portion of the solar spectrum and achieved remarkable photovoltaic cell performance (Nazerruddin et al., 1993; O' Regan & Gratzel, 1991; Smestad & Gratzel, 1998). Nanoporosity of the  $\text{TiO}_2$  paste (or colloidal solution) is achievable by sintering (annealing) of the deposited  $\text{TiO}_2$  layer at approximately  $450^\circ\text{C}$  in a well ventilated zone for about 15 minutes (see Figure 4). The high porosity (>50%) of the nanostructured  $\text{TiO}_2$  layer allows facile diffusion of redox mediators within the layer to react with surface-bound sensitizers. Lindström et al. reported "A method for manufacturing a nanostructured porous layer of a semiconductor material at room temperature. The porous layer is pressed on a conducting glass or plastic substrate for use in a dye-sensitized nanocrystalline solar cell." (Lindström et al., 2001)

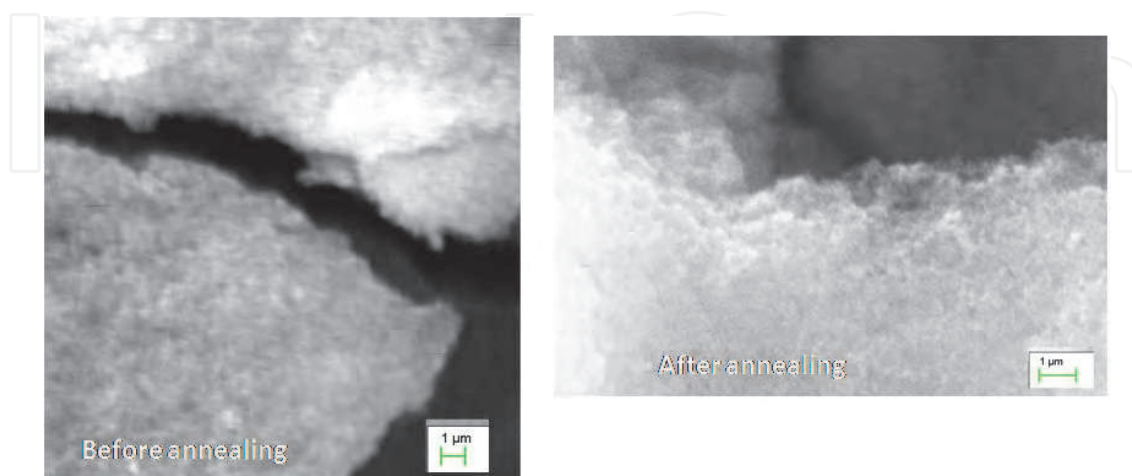


Fig. 4. Scanning electron microscope (SEM) images for  $\text{TiO}_2$  photoelectrode before and after annealing it at about  $450^\circ\text{C}$  for 15 minutes.

Because it is not expensive, none toxic and having good chemical stability in solution while irradiated, Titanium dioxide has attracted great attention in many fields other than nanostructured photovoltaics such as photocatalysts, environmental purification, electronic devices, gas sensors, and photoelectrodes (Karami, 2010). The preparation procedures of  $\text{TiO}_2$  film is quite simple since it requires no vacuum facilities. Nanostructured  $\text{TiO}_2$  layers are prepared following the procedure detailed in (Hara & Arakawa, 2003; Nazerruddin et al., 1993; O' Regan & Gratzel, 1991; Smestad, 1998) "A suspension of  $\text{TiO}_2$  is prepared by adding 9 ml of nitric acid solution of PH 3-4 (1 ml increment) to 6 g of colloidal P25  $\text{TiO}_2$  powder in mortar and pestle. While grinding, 8 ml of distilled water (in 1 ml increment) is added to get a white- free flow- paste. Finally, a drop of transparent surfactant is added in 1 ml of distilled water to ensure coating uniformity and adhesion to the transparent conducting glass electrode. The ratio of the nitric acid solution to the colloidal P25  $\text{TiO}_2$  powder is a critical factor for the cell performance. If the ratio exceeds a certain threshold value the resulting film becomes too thick and has a tendency to peel off. On the other hand, a low ratio reduces appreciably the efficiency of light absorption" (Jasim & Hassan, 2009). Our group adopted the Doctor blade method to deposit  $\text{TiO}_2$  suspension uniformly on a cleaned (rinsed with ethanol) electrode plate. The  $\text{TiO}_2$  layer must be allowed to dry for few minutes and then annealed at approximately  $450^\circ\text{C}$  (in a well ventilated zone) for about 15 minutes to form a nanoporous, large surface area  $\text{TiO}_2$  layer. The nanostructured film must be allowed to cool down slowly to room temperature. This is a necessary condition to remove thermal stresses and avoid cracking of the glass or peeling off the  $\text{TiO}_2$  film.

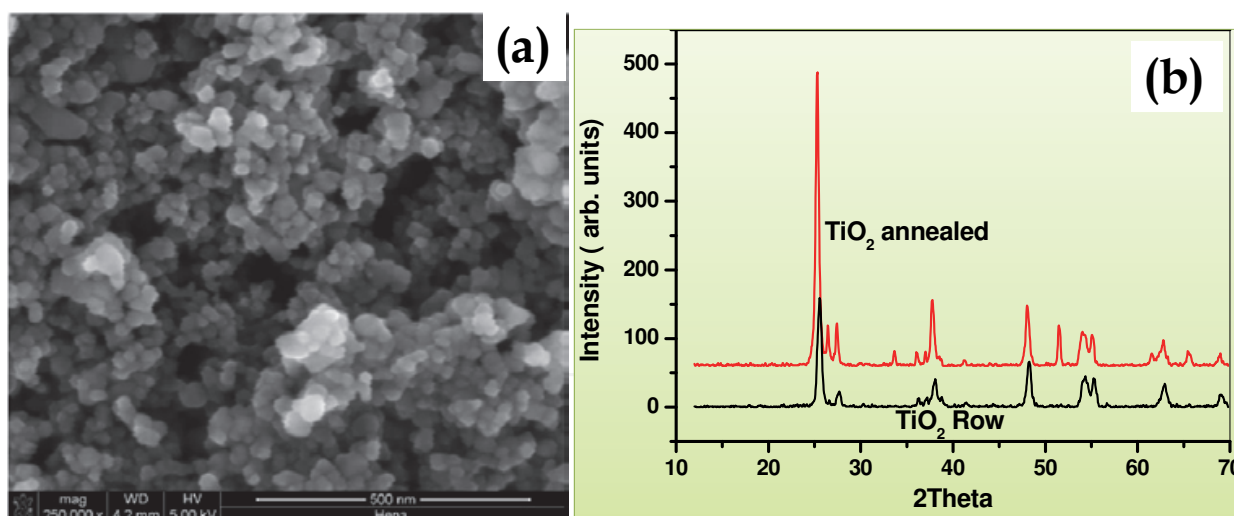


Fig. 5. (a) Scanning electron microscope (SEM) images and (b) XRD for  $\text{TiO}_2$  photoelectrode before and after being annealed.

Scanning electron microscopy SEM (see Figure 5-a) or X-ray diffraction measurements (XRD) (see Figure 5-b) is usually used to confirm the formation of nanostructured  $\text{TiO}_2$  layer. Analysis of the XRD data (shown in Figure 5-b) confirms the formation of nanocrystalline  $\text{TiO}_2$  particles of sizes less than 50 nm (Jasim & Hassan, 2009). The nanoporous structure of the  $\text{TiO}_2$  layer suggests that the roughness factor of 1000 is achievable. In other words, a  $1\text{-cm}^2$  coated area of the conductive transparent electrode with nanostructured  $\text{TiO}_2$  layer actually possessing a surface area of  $1000\text{ cm}^2$  (Hara & Arakawa, 2003). The formation of nanostructured  $\text{TiO}_2$  layer is greatly affected by  $\text{TiO}_2$  suspension



preparation procedures as well as by the annealing temperature. We found that a sintered  $\text{TiO}_2$  film at temperatures lower than the recommended  $450^\circ\text{C}$  resulted in cells that generate unnoticeable electric current even in the  $\mu\text{A}$  level. Moreover, nanostructured  $\text{TiO}_2$  layer degradation in this case is fast and cracks form after a short period of time when the cell is exposed to direct sunlight. Recently Zhu et al. investigated the effects of annealing temperature on the charge-collection and light-harvesting properties of  $\text{TiO}_2$  nanotube-based dye-sensitized solar cells (see Figure 6) and the reported “DSSCs containing titanium oxide nanotube (NT) arrays films annealed at  $400^\circ\text{C}$  exhibited the fastest transport and slowest recombination kinetics. The various structural changes were also found to affect the light-harvesting, charge-injection, and charge-collection properties of DSSCs, which, in turn, altered the photocurrent density, photovoltage, and solar energy conversion efficiency” (Zhu et al. 2010).

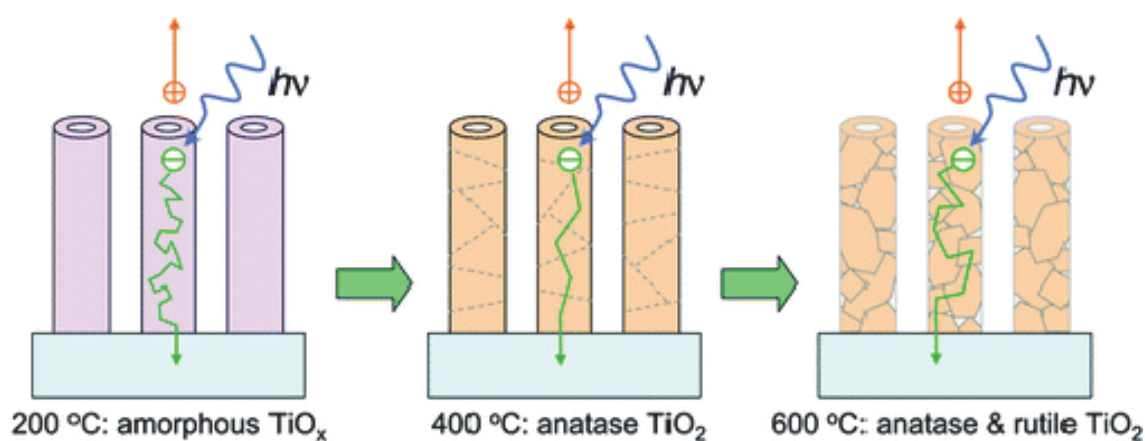


Fig. 6. Schematic illustration of the effects of annealing temperature on the charge-collection and light-harvesting properties of  $\text{TiO}_2$  nanotube-based dye-sensitized solar cells (From Zhu et al., 2010).

One of the important factors that affect the cell's efficiency is the thickness of the nanostructured  $\text{TiO}_2$  layer which must be less than  $20\ \mu\text{m}$  to ensure that the diffusion length of the photoelectrons is greater than that of the nanocrystalline  $\text{TiO}_2$  layer.  $\text{TiO}_2$  is the most commonly used nanocrystalline semiconductor oxide electrode in the DSSC as an electron acceptor to support a molecular or quantum dot QD sensitizer is  $\text{TiO}_2$  (Gratzel, 2003). Other wide bandgap semiconductor oxides becoming common is the zinc oxide  $\text{ZnO}$ .  $\text{ZnO}$  possesses a bandgap of  $3.37\ \text{eV}$  and a large excitation binding energy of  $60\ \text{meV}$ . Kim *et al.* reported that the nanorods array electrode showed stable photovoltaic properties and exhibited much higher energy conversion efficiency (Kim et al., 2006). Another example, Law and coworkers have grown by chemical bath deposition  $\text{ZnO}$  nanowires  $8\text{-}\mu\text{m}$  long with  $100\ \text{nm}$  diameters as photoelectrode (see Figure 7) the efficiency of a  $\text{ZnO}$  nanowire photoelectrode DSSC is about  $2.4\%$ . This low efficiency level compared to that of nanostructured  $\text{TiO}_2$  photoelectrode DSSC is probably due to inadequate surface area for sensitizer adsorption (Baxter et al., 2006; Boercker et al., 2009; Law et al., 2005). Other research groups suggested that the growth of longer, thinner, denser  $\text{ZnO}$  nanowires is a practical approach to enhance cell efficiency (Guo et al., 2005). Investigations show that  $\text{ZnO}$  nanorod size could be freely modified by controlling the solution conditions such as temperature, precursor concentration, reaction time, and adopting multi-step growth. Nanorod structured photoelectrode offers a great potential for improved electron transport.

It has been found that the short circuit current density and cell performance significantly increase as nanorods length increases because a higher amount of the adsorbed dye on longer nanorods, resulting in improving conversion efficiency (Kim et al. 2006).

Because titanium dioxide is abundant, low cost, biocompatible and non-toxic (Gratzel & Hagfeldt, 2000), it is advantageous to be used in dye sensitized solar cells. Therefore, nanotube and nanowire-structured  $\text{TiO}_2$  photoelectrode for dye-sensitized solar cells have been investigated (Mor et al., 2006; Pavasupree et al., 2005; Pavasupree et al., 2006; Shen et al., 2006; Suzuki et al., 2006). Moreover,  $\text{SnO}_2$ , or  $\text{Nb}_2\text{O}_5$  employed not only to ensure large roughness factor (after nanostructuring the photoelectrode) but also to increase photogenerated electron diffusion length (Bergeron et al., 2005; Sun et al. 2006). Many studies suggest replacing nanoparticles film with an array of single crystalline nanowires (rods), nanoplants, or nanosheets in which the electron transport increases by several orders of magnitude (Kopidakis et al., 2003; Law et al., 2005; Noack et al., 2002; Tiwari & Snure, 2008; Xian et al., 2006). Incorporation of vertically aligned carbon nanotube counter electrode improved efficiency of  $\text{TiO}_2$ /anthocyanin dye-Sensitized solar cells as reported by Sayer et al. They attributed the improvement to “the large surface area created by the 3D structure of the arrays in comparison to the planar geometry of the graphite and Pt electrodes, as well as the excellent electrical properties of the CNTs.” (Sayer et al., 2010).

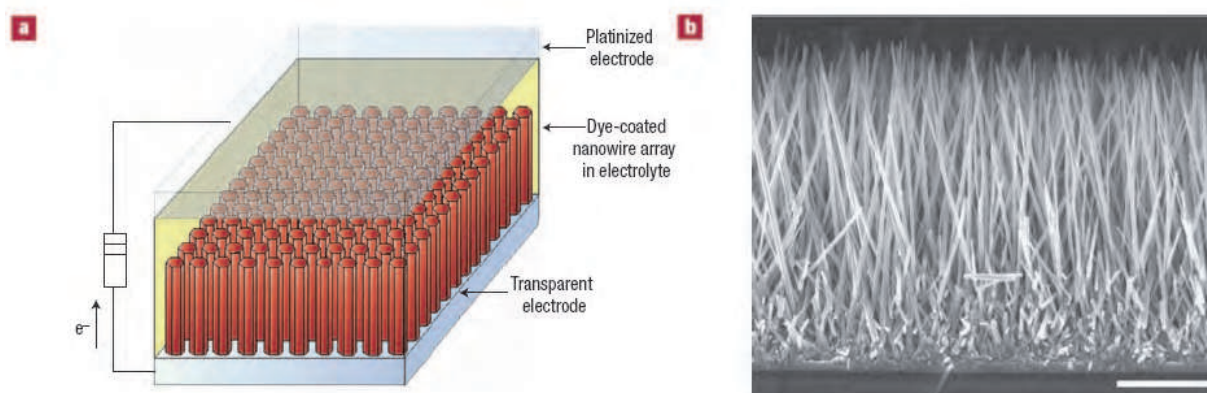


Fig. 7. (a) Schematic illustration of the ZnO nanowire dye sensitized solar cell, light is incident through the bottom electrode, and (b) scanning electron microscopy cross-section of a cleaved nanowire array. The wires are in direct contact with the transparent substrate, with no intervening particle layer. Scale bar, 5- $\mu\text{m}$  (From Law et al., 2005).

### 2.3 Photosensitizer

Dye molecules of proper molecular structure are used to sensitize wide bandgap nanostructured photoelectrode. Upon absorption of photon, a dye molecule adsorbed to the surface of say nanostructured  $\text{TiO}_2$  gets oxidized and the excited electron is injected into the nanostructured  $\text{TiO}_2$ . Among the first kind of promising sensitizers were Polypyridyl compounds of Ru(II) that have been investigated extensively. Many researches have focused on molecular engineering of ruthenium compounds. Nazeeruddin et al. have reported the “black dye” as promising charge transfer sensitizer in DSSC. Kelly, et al. studied other ruthenium complexes  $\text{Ru}(\text{dcb})(\text{bpy})_2$  (Kelly, et al 1999), Farzad et al. explored the  $\text{Ru}(\text{dcbH}_2)(\text{bpy})_2(\text{PF}_6)_2$  and  $\text{Os}(\text{dcbH}_2)(\text{bpy})_2(\text{PF}_6)_2$  (Farzad et al., 1999), Qu et al. studied *cis*- $\text{Ru}(\text{bpy})_2(\text{ina})_2(\text{PF}_6)_2$  (Qu et al., 2000), Shoute et al.

investigated the *cis*-Ru(dcbH<sub>2</sub>)<sub>2</sub>(NCS) (Shoute et al., 2003), and Kleverlaan et al. worked with OsIII-bpa-Ru (Kleverlaan et al 2000). Sensitizations of natural dye extracts such as shiso leaf pigments (Kumara et al., 2006), Black rice (Hao et al., 2006), Fruit of calafate (Polo and Iha, 2006), Rosella (Wongcharee et al., 2007), Natural anthocyanins (Fernando et al., 2008), Henna (*Lawsonia inermis* L.) (Jasim & Hassan, 2009; Jasim et al., in press 2011), and wormwood, bamboo leaves (En Mei Jin *et al.*, 2010) have been investigated and photovoltaic action of the tested cells reveals some opportunities. Calogero et al. suggested that “Finding appropriate additives for improving open circuit voltage  $V_{oc}$  without causing dye degradation might result in a further enhancement of cell performance, making the practical application of such systems more suitable to economically viable solar energy devices for our society.” (Calogero et al., 2009)

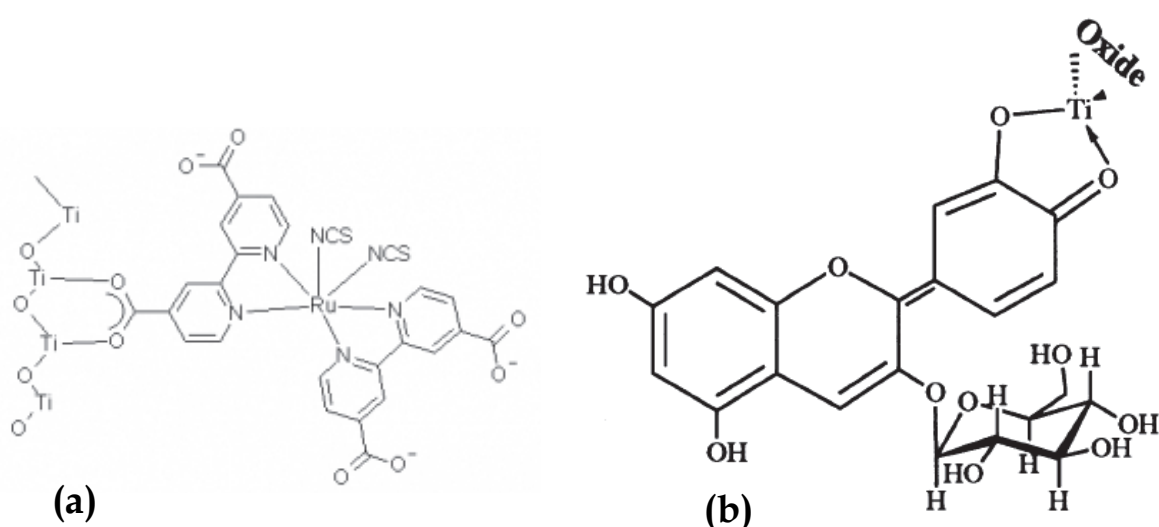


Fig. 8. (a) Ruthenium based red or "N3" dye adsorbed onto a titanium dioxide surface (from Martinson et al., 2008), and (b) Proposed structure of the cyanin dye adsorbed to one of the titanium metal centers on the titanium dioxide surface (From Smestad, 1988).

Gratzel group developed many Ru complex photosensitizers (examples are shown in Figure 16). One famous example is the *cis*-Di(thiocyanato)bis(2,2'-bipyridyl)-4,4'-dicarboxylate ruthenium(II), coded as N3 or N-719 dye it has been an outstanding solar light absorber and charge-transfer sensitizer. The red dye or N3 dye (structure is shown in Figure 8-a and Figure 16) is capable of absorbing photons of wavelength ranging from 400 nm to 900 nm (see Figure 16) because of metal to ligand charge transfer transition. Theoretical Study of new ruthenium-based dyes for dye sensitized solar cells by Monari et al., states “The UV/vis absorption spectra have been computed within the time-dependent density functional theory formalism. The obtained excitation energies are compared with the experimental results.” (Monari et al., 2011) In fact, for dye molecule to be excellent sensitizer, it must possess several carbonyl (C=O) or hydroxyl (-OH) groups capable of chelating to the Ti<sup>(IV)</sup> sites on the TiO<sub>2</sub> surface as shown in Figure 8 (Tennakone et al., 1997). Extracted dye from California blackberries (*Rubus ursinus*) has been found to be an excellent fast-staining dye for sensitization, on the other hand, dyes extracted from strawberries lack such complexing capability and hence not suggested as natural dye sensitizer (Cherpy et al., 1997; Semistad & Gratzel, 1998; Semistad, 1988).

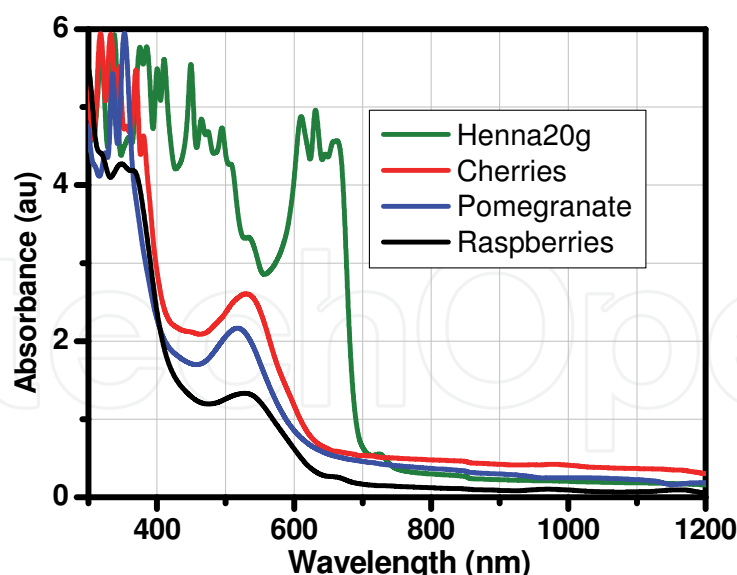


Fig. 9. Measured absorbance of some extracted natural dyes in methanol as solvent.

Commercialized dye sensitized solar cells and modules use ruthenium bipyridyl-based dyes (N3 dyes or N917) achieved conversion efficiencies above 10% (Nazerruddin, et al., 1993). However, these dyes and those chemically engineered are hard to put up and are expensive (Cherepy et al., 1997). Therefore, in attempt to develop green solar cells; our group at the University of Bahrain used Soxhlet Extractor in the extraction of natural dye solutions from abundant natural dye sources such as Bahraini Henna (*Lawsonia inermis* L.), Yemeni Henna, pomegranate, raspberries, and cherries after being dried (Jasim, submitted for publication 2011). We used methanol as solvent in each extraction process. The absorbance of the extracted dye solution has been measured using dual beam spectrophotometer (see Figure 9). Different concentrations of Henna (*Lawsonia inermis* L.) extracts have been prepared from the original extract. The light harvesting efficiency (LHE) for each concentration has been calculated from the absorbance (see Figure 10). The light harvesting efficiency is given as:

$$LHE(\lambda) = (1 - 10^{-A(\lambda)}) \times 100 \quad (1)$$

where  $A(\lambda)$  is the absorbance of the sample at specific wavelength.

The absorbance and hence the LHE increases with concentration of dye extract. Also, as shown in Figure 10, as Henna extract concentration increases the absorbance increases and covers broader range of wavelengths.

Since not all photons scattered by or transmitted through the nanocrystalline  $\text{TiO}_2$  layer get absorbed by a monolayer of the adsorbed dyes molecules, the incorporation of energy relay dyes might help enhancing the light harvesting efficiency. A remarkable enhancement in absorption spectral bandwidth and 26% increase in power conversion efficiency have been accomplished with some sensitizers after energy relay dyes have been added (Harding et al., 2009). Metal free organic sensitizers such as metal free iodine reported by Horiuchi et al. demonstrated remarkable high efficiency "The solar energy to current conversion efficiencies with the new indoline dye was 6.51%. Under the same conditions, the N3 dye was 7.89%" (Horiuchi et al., 2004). Semiconductor quantum dots QDs are nanostructured crystalline semiconductors where quantum confinement effect due to their size results in

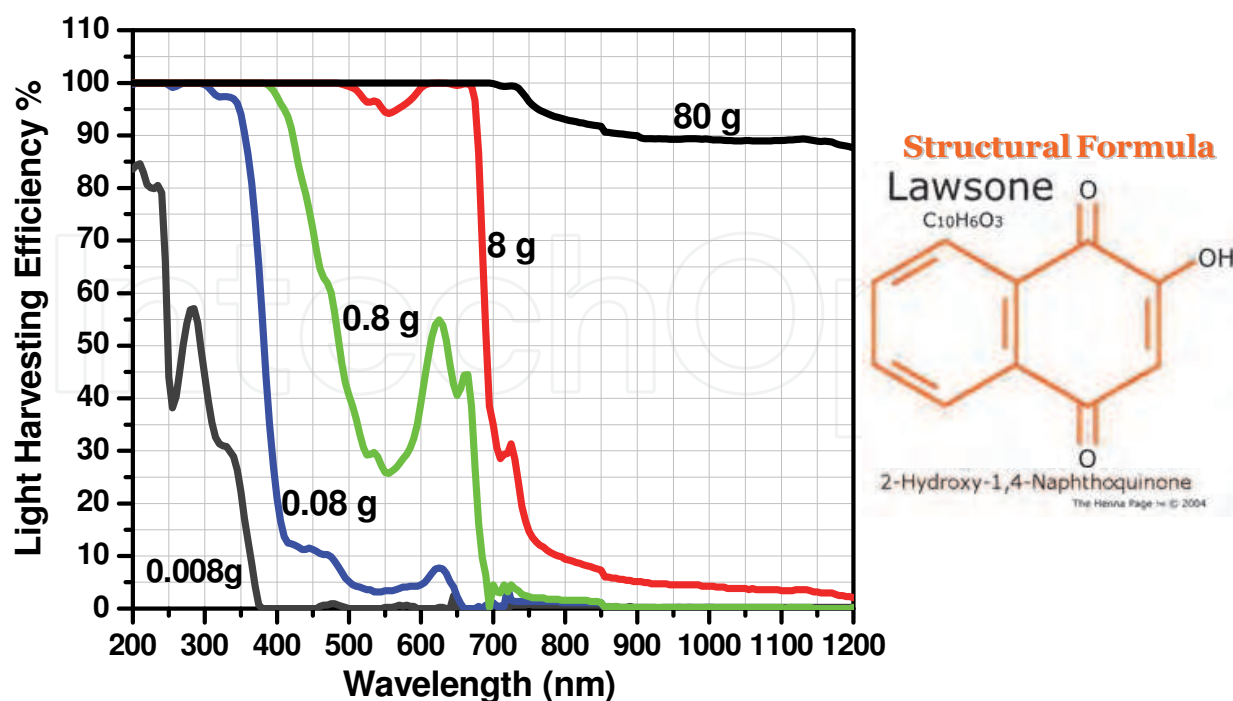


Fig. 10. Light harvesting efficiency of Henna extract at different concentrations. Data are given in grams of Henna powder per 100 ml of methanol as solvent. Also, shown the structural formula of Lawsone molecule that is responsible for the characteristic color of Henna (From [www.hennapage.com](http://www.hennapage.com)).

remarkable optical linear and nonlinear behaviors. Excitonic absorption edge of quantum dots is size dependent as shown in Figure 11 for lead sulfide PbS quantum dots suspended in toluene. It is anticipated that quantum dots are alternatives of dyes as light-harvesting structures in DSSC. Light absorption produces excitons or electron-hole pairs. Excitons have an average physical separation between the electron and hole, referred to as the Exciton Bohr Radius. Usually, Bohr radius is greater the QD diameter (e.g., for PbS Bohr radius is 20 nm) leading to quantum confinement effect (discrete energy levels = artificial molecule). Excitons dissociate at the QD TiO<sub>2</sub> interface. The electron is subsequently injected in the semiconductor oxide conduction band, while the hole is transferred to a hole conductor or an electrolyte. Efficient and rapid hole injection from PbS QDs into triarylamine hole conductors has been demonstrated, and IPCE (Incident Photon to Current Conversion Efficiency) values exceeding 50% have been obtained. QDs have much higher optical cross sections than molecular sensitizers, depending on their size. However, they also occupy a larger area on the surface of the nanostructured photoelectrode, decreasing the QD concentration in the film. Thus, the value of the absorption length is similar to that observed for the dye-loaded nanostructured photoelectrode. Investigations show that multiple excitons can be produced from the absorption of a single photon by a QD via impact ionization if the photon energy is 3 times higher than its band gap (Ellinson et al., 2005; Nozik, 2004; Nozik, 2005). The issue to be confronted is to find ways to collect the excitons before they recombine get lost in the cell.

Unlike dyes that absorb over relatively narrow region, semiconductor quantum dots such as PbS (see Figure 11-b) absorb strongly all photons with energy greater than the bandgap,

thus a far higher proportion of light can be converted into useful energy using nanocrystals compared to dyes. Perhaps most important, dyes are disgracefully unstable and tend to photobleach over a relatively short amount of time. Quantum dots prepared with a properly designed outer shell are very stable and hence long lasting solar cells without degradation in performance are feasible. Quantum dots-sensitized solar cell produces quantum yields greater than one due to impact ionization process (Nozik, 2001). Dye molecules cannot undergo this process. Solar cells made from semiconductor QDs such as CdSe, CdS, PbS and InP showed a promising photovoltaic effect (Hoyer & Konenkamp, 1995; Liu & Kamat 1993; Plass et al., 2002; Vogel & Weller 1994; Zaban et al., 1998; Zweible & Green, 2000). Significant successes have been achieved in improving the photo-conversion efficiency of solar cells based on CdSe quantum dot light harvesters supported with carbon nanotube this is accomplished by incorporating carbon nanotubes network in the nanostructured TiO<sub>2</sub> layer, and accordingly assisting charge transport process network (Hasobe et al., 2006; Robel et al., 2005). Consequently, appreciable improvement in the photo-conversion efficiency of the DSSC is attainable. Recently Fuke et al., reported CdSe quantum-dot-sensitized solar cell with ~100% internal quantum efficiency. A significant enhancement in both the electron injection efficiency at the QD/TiO<sub>2</sub> interface and charge collection efficiency at the QD/electrolyte interface" were achieved (Fuke et al., 2010).

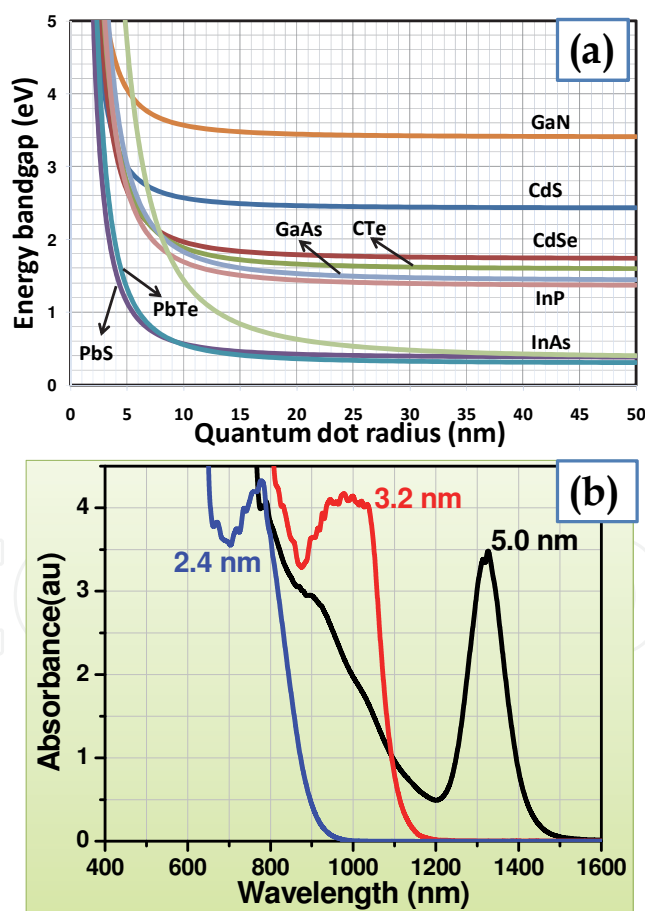


Fig. 11. (a) Calculated energy gap of some semiconductor quantum dots using the effective mass-approximation-model and (b) measured absorbance of PbS quantum dots suspended in toluene of three different sizes (radius).

## 2.4 Redox electrolyte

Electrolyte containing  $I^-/I_3^-$  redox ions is used in DSSC to regenerate the oxidized dye molecules and hence completing the electric circuit by mediating electrons between the nanostructured electrode and counter electrode. NaI, LiI and  $R_4NI$  (tetraalkylammonium iodide) are well known examples of mixture of iodide usually dissolved in nonprotic solvents such as acetonitrile, propylene carbonate and propionitrile to make electrolyte. Cell performance is greatly affected by ion conductivity in the electrolyte which is directly affected by the viscosity of the solvent. Thus, solvent with lower viscosity is highly recommended. Moreover, counter cations of iodides such as  $Na^+$ ,  $Li^+$ , and  $R_4N^+$  do affect the cell performance mainly due to their adsorption on nanostructured electrode ( $TiO_2$ ) or ion conductivity. It has been found that addition of *tert*-butylpyridine to the redoxing electrolyte improves cell performance (Nazeeruddin et al., 1993) (see Figure 19).  $Br^-/Br_3^-$  redox couple was used in DSSCs and promising results were obtained. The  $V_{oc}$  and  $I_{sc}$  increased for the Eosin Y-based DSSC when the redox couple was changed from  $I^-/I_3^-$  to  $Br^-/Br_3^-$  (Suri & Mehra, 2006).

The redoxing electrolyte needs to be chosen such that the reduction of  $I_3^-$  ions by injection of electrons is fast and efficient (see Figure 13). This arises from the fact that the dependence of both hole transport and collection efficiency on the dye-cation reduction and  $I^-/I_3^-$  redox efficiency at counter electrodes are to be taken into account (Yanagida, 2006). Besides limiting cell stability due to evaporation, liquid electrolyte inhibits fabrication of multi-cell modules, since module manufacturing requires cells be connected electrically yet separated chemically (Matsumoto et al., 2001; Tennakone et al., 1999). Hence, a significant shortcoming of the dye sensitized solar cells filled with liquid state redoxing electrolyte is the leakage of the electrolyte, leading to reduction of cell's lifespan, as well as the associated technological problems related to device sealing up and hence, long-term stability (Kang, et al., 2003). Many research groups investigate the use of ionic liquids, polymer, and hole conductor electrolytes (see Figure 12) to replace the need of organic solvents in liquid electrolytes. Despite the reported relative low cell's efficiency of 4–7.5% (device area  $< 1\text{ cm}^2$ ), these kind of electrolyte are promising and may facilitate commercialization of dye sensitized solar modules (Kawano, et al., 2004; Kuang et al., 2006; Schmidt-Mende & Gratzel, 2006; Wang et al., 2004).

Addition of polymer gel to quasi-solidify electrolytes has been investigated by many research groups (Ren et al., 2001; Kubo et al., 2001; Nogueira et al., 2001). It has been found that the addition of Poly(vinylidene fluoride-co-hexafluoropropylene) to the  $KI/I_2$  electrolyte has improved both the fill factors and energy conversion efficiency of the cells by about 17% (Kang, et al., 2003). Gel electrolytes also are very attractive from many perspectives such as: Efficiency is a compromise between electrolyte viscosity and ionic mobility; gelled ionic liquids have an anomalously high ionic mobility despite their high viscosity, and particularly for realization of monolithic arrays inter-cell sealing (Wang, et al., 2005). Innovative classes of electrolytes such as p-type, polymeric conductor, PEDOT or PEDOT:TMA, which carries electrons from the counter electrode to the oxidized dye encouraging further investigations to optimize and/or design new ones. Recently one of the first systematic study of charge transport and recombination in solid state dye sensitized solar cell SDSCs using conjugated polymer hole transporter has been reported by Zhang et al., in this investigation organic indoline dye D131 as the sensitizer and poly(3-hexylthiophene) (P3HT) as the hole transporter a power conversion efficiency of 3.85% have been recorded. Therefore, this class of solar cells is expected to represent one of the most efficient SDSCs using polymeric hole transporter (Zhang et al, 2011).

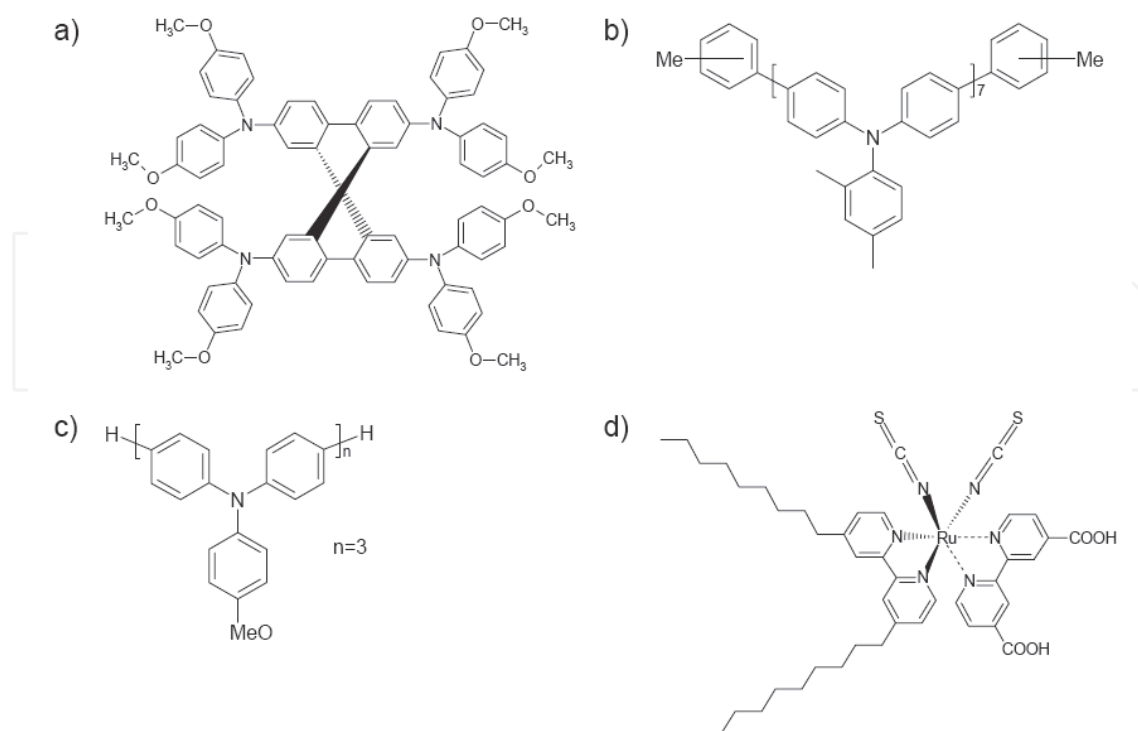


Fig. 12. (a) Chemical structure of the hole-conductor spiro-OMeTAD resulted in cells energy conversion efficiency  $\eta = 4\%$ , (b) Chemical structure of AV-DM resulted in cells with  $\eta = 0.9\%$ , (c) Structure of AV-OM. resulted in cells with  $\eta = 2\%$ , (d) Structure of the Z907 dye used for all solar cells as sensitizer of the nanostructured TiO<sub>2</sub> film (From Schmidt-Mende & Gratzel, 2006).

### 3. How dye sensitized solar cell works

In this section we overview the following: Process during which light energy get converted to electric one, photovoltaic performance, charge injection, charge transport in the nanostructured electrode, charge recombination, and cell dark current.

#### 3.1 Operating principle of dye sensitized solar cell

Nanocrystalline TiO<sub>2</sub> is deposited on the conducting electrode (photoelectrode) to provide the necessary large surface area to adsorb sensitizers (dye molecules). Upon absorption of photons, dye molecules are excited from the highest occupied molecular orbitals (HOMO) to the lowest unoccupied molecular orbital (LUMO) states as shown schematically in Figure 13. This process is represented by Eq. 2. Once an electron is injected into the conduction band of the wide bandgap semiconductor nanostructured TiO<sub>2</sub> film, the dye molecule (photosensitizer) becomes oxidized, (Equation 3). The injected electron is transported between the TiO<sub>2</sub> nanoparticles and then extracted to a load where the work done is delivered as an electrical energy, (Equation 4). Electrolytes containing I<sup>-</sup>/I<sub>3</sub><sup>-</sup> redox ions is used as an electron mediator between the TiO<sub>2</sub> photoelectrode and the carbon coated counter electrode. Therefore, the oxidized dye molecules (photosensitizer) are regenerated by receiving electrons from the I<sup>-</sup> ion redox mediator that get oxidized to I<sub>3</sub><sup>-</sup> (Tri-iodide ions). This process is represented by Eq. 5. The I<sub>3</sub><sup>-</sup> substitutes the internally donated electron



with that from the external load and reduced back to  $I^-$  ion, (Equation 6). The movement of electrons in the conduction band of the wide bandgap nanostructured semiconductor is accompanied by the diffusion of charge-compensating cations in the electrolyte layer close to the nanoparticle surface. Therefore, generation of electric power in DSSC causes no permanent chemical change or transformation (Gratzel, 2005).

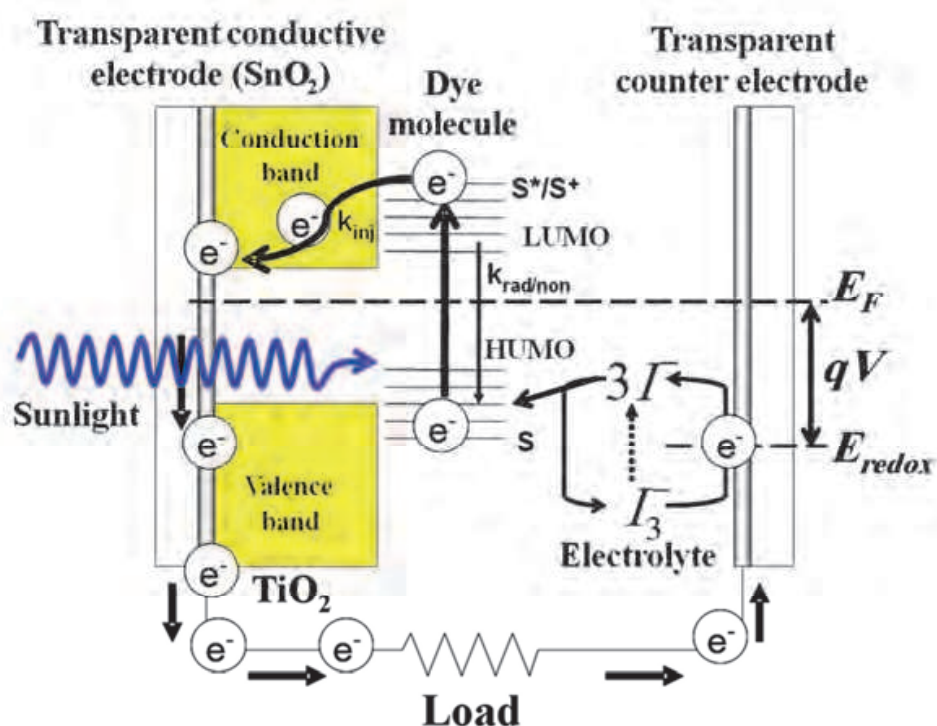


Fig. 13. Schematic illustration of operation principle of dye sensitized solar cell.

As illustrated in Fig. 13, the maximum potential produced by the cell is determined by the energy separation between the electrolyte chemical potential ( $E_{\text{redox}}$ ) and the Fermi level ( $E_F$ ) of the  $\text{TiO}_2$  layer. The small energy separation between the HOMO and LUMO ensures absorption of low energy photons in the solar spectrum. Therefore, the photocurrent level is dependent on the HOMO-LUMO levels separation. This is analogous to inorganic

semiconductors energy bandgap ( $E_g$ ). In fact, effective electron injection into the conduction band of  $\text{TiO}_2$  is improved with the increase of energy separation of LUMO and the bottom of the  $\text{TiO}_2$  conduction band. Furthermore, for the HOMO level to effectively accept the donated electrons from the redox mediator, the energy difference between the HOMO and redox chemical potential must be more positive (Hara & Arakawa, 2003).

### 3.2 Photovoltaic performance

Figure 14 presents examples of the I-V characteristics of natural dye sensitized solar cell NDSSC with Bahraini Henna (*Lawsonia inermis* L.), pomegranate, Bahraini raspberries, and cherries. We found that nature of the dye and its concentration has a remarkable effect on the magnitude of the collected photocurrent. Under full solar spectrum irradiation with photon flux  $I_0 = 100 \text{ mW/cm}^2$  (Air Mass 1.5), the photon energy -to- electricity conversion efficiency is defined as (Gratzel, 2003):

$$\eta = \frac{J_{sc} \times V_{oc} \times FF}{I_0} \quad (7)$$

where  $J_{sc}$  is the short circuit current,  $V_{oc}$  the open circuit voltage, and FF is the fill factor of the solar cell which is calculated by multiplying both the photocurrent and voltage resulting in maximum electric power delivered by the cell.

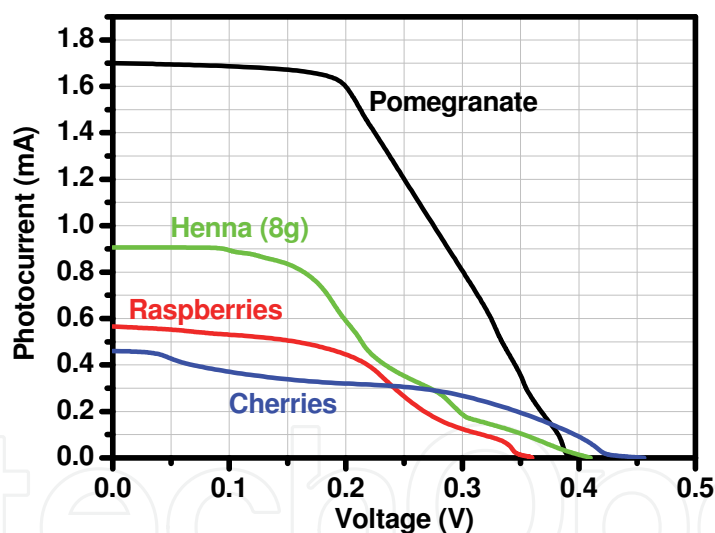


Fig. 14. Photocurrent vs. voltage curves obtained for nanostructured  $\text{TiO}_2$  photoelectrodes sensitized with some extracted natural dyes (Jasim, submitted for publications).

Table 3 shows the electrical properties of some assembled NDSSCs. Photocurrent and voltage drop on a variable load have been recorded instantaneously while the cell is exposed to direct sun illumination. Due to light reflection and absorption by the conductive photoelectrode and the scattering nature of the nanostructured  $\text{TiO}_2$ , the measured transmittance of the photoelectrode (see Figure 3) shows an average of 10% of the solar spectrum (Air Mass 1.5) may reach the sensitizers. Since  $\text{TiO}_2$  past is applied on the conductive electrode using doctor blade method the effective area of the irradiated part of the cell is  $1.5 \text{ cm} \times 2 \text{ cm}$ . Despite the variation of Bahraini Henna extract concentration the cells produced almost the same open circuit voltage  $V_{oc}$ . On the other hand, the short circuit

current  $I_{sc}$  varies with Henna extract concentration. Highly concentrated Bahraini Henna extracts results in non-ideal I-V characteristics even though it possesses 100% light harvesting efficiency in the UV and in the visible parts of the electromagnetic spectrum. The dye concentration was found to influence remarkably the magnitude of the collected photocurrent. High concentration of Henna extract introduces a series resistance that ultimately reduces the generated photocurrent. On the other hand, diluted extracts reduces the magnitude of the photocurrent and cell efficiency. (Jasim et al, 2011).

Dye	$V_{oc}$ (V)	$I_{sc}$ (mA)	FF	% $\eta$
Bahraini Henna 80g	0.426	0.368	0.246	0.128
Bahraini Henna 8g	0.410	0.906	0.363	0.450
Bahraini Henna 0.8g	0.419	0.620	0.330	0.286
Yameni Henna 84g	0.306	0.407	0.281	0.117
Yameni Henna 21g	0.326	0.430	0.371	0.174
Yameni Henna 4.2g	0.500	0.414	0.276	0.191
Cherries in Methanol	0.305	0.466	0.383	0.181
Cherries in Methanol+ 1% HCL	0.301	0.463	0.288	0.134
Pomegranate	0.395	1.700	0.481	1.076
Raspberries	0.360	0.566	0.455	0.309

Table 3. Electrical properties of some assembled natural dye sensitized solar cells NDSSCs (From Jasim et al, 2011; Jasim, submitted for publications).

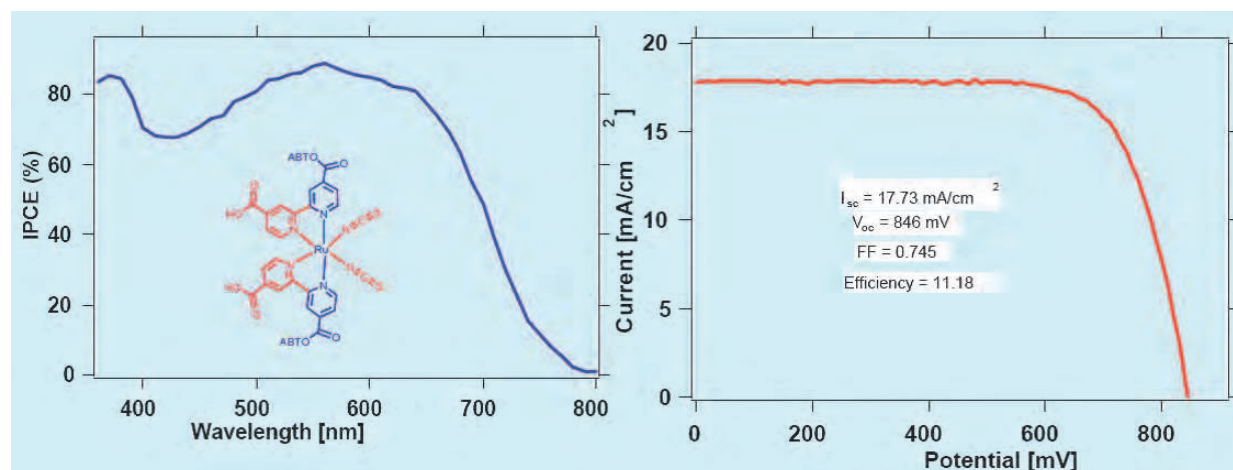


Fig. 15. Photovoltaic performance of DSSC laboratory cell (a) Photo current action spectrum showing the monochromatic incident photon to current conversion efficiency (IPCE) as function of light wavelength obtained with the N-719 sensitizer. (b) Photocurrent density – voltage curve of the same cell under AM 1.5 standard test conditions. (From Nazeeruddin et al., 2005).

Gratzel and coworkers reported cell efficiency of 10.4% using black dye ( $RuL'(NCS)_3$  complexes) and as shown in Figure 15, cells with solar to electric power conversion efficiency of the DSSC in full AM 1.5 sun light validated by accredited PV calibration laboratories has reached over 11% (Chiba et al., 2006). Jiu et al., (Jiu, et al., 2006) have

synthesized highly crystalline TiO<sub>2</sub> nanorods with lengths of 100-300 nm and diameters of 20-30 nm. The rod shape kept under high calcination temperatures contributed to the achievement of the high conversion efficiency of light-to-electricity of 7.29%. Reported efficiencies of nanostructured ZnO<sub>2</sub> photoelectrodes based cells are encouraging and many research groups are dedicating their efforts to provide cells with efficiency close to that reported for sensitized nanostructured TiO<sub>2</sub> photoelectrodes.

The short circuit current magnitude affects directly the incident photon-to-current conversion efficiency IPCE which is defined using the photoresponse and the light intensity as:

$$IPCE(\lambda) = \frac{1240(eV \cdot nm) \times J_{sc} (\mu A / cm^2)}{\lambda(nm) \times I(\mu W / cm^2)} \quad (8)$$

where  $\lambda$  is the wavelength of the absorbed photon and  $I$  is the light intensity at wavelength  $\lambda$ . Figures 15 and 16 present IPCE examples of some commonly used sensitizers by Gratzel and coworkers.

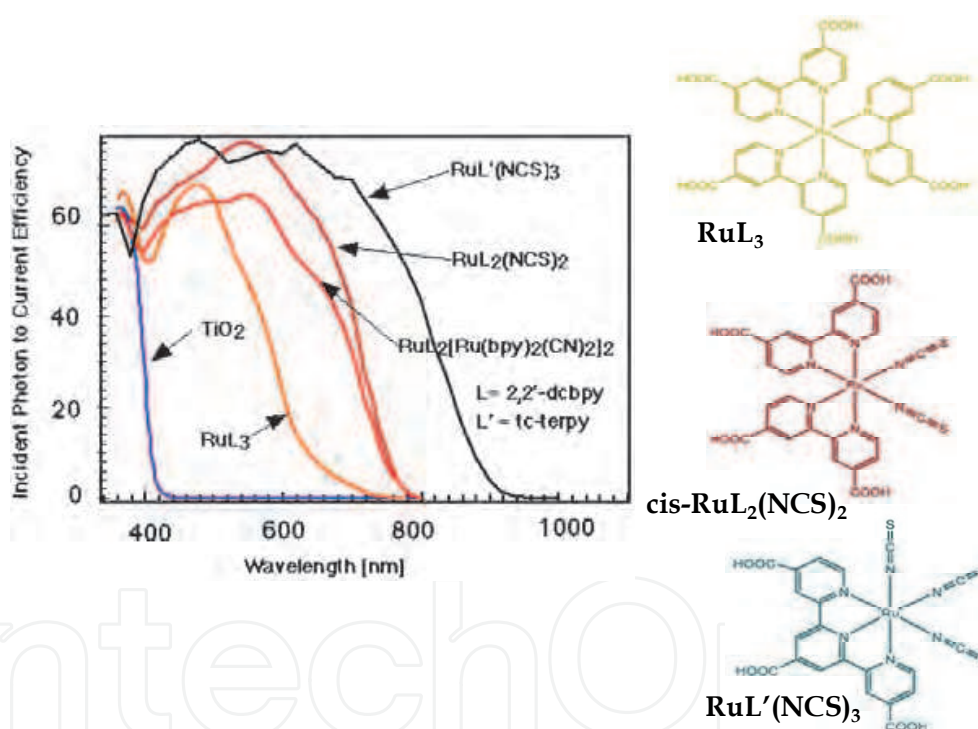


Fig. 16. Spectral response (IPCE) of dye-sensitized solar cell for different dyes compared with the spectral response of bare TiO<sub>2</sub> electrode and the ideal IPCE curve for a single bandgap device (From <http://dcwww.epfl.ch/icp/ICP-2/solarcellE.html>. and Gratzel et al., 2005).

In terms of light harvesting efficiency LHE, quantum yield of electron injection quantum yield  $\Phi_{inj}$ , and collection efficiency  $\eta_c$  of the injected electrons at the back contact IPCE is given by:

$$IPCE = LHE \times \Phi_{inj} \times \eta_c \quad (9)$$

Therefore, IPCE equals the LHE if both  $\Phi_{inj}$  and  $\eta_c$  are close 100%. However, Charge injection from the electronically excited sensitizer into the conduction band of the nanostructured wide bandgap semiconductor is in furious competition with other radiative and non-radiative processes. Due to electron transfer dynamics (see Figure 17), if electron injection in the semiconductor is comparable to, or slower than, the relaxation time of the dye,  $\Phi_{inj}$  will be way below 100%. This can be deduced from the definition of the quantum yield  $\Phi_{inj}$  (Cherepy et al., 1997):

$$\Phi_{inj} = \frac{k_{inj}}{k_{inj} + k_{rad} + k_{nrad}} \quad (10)$$

The quantum yield approaches 100% only when the radiative and nonradiative rates ( $k_{rad}$ ,  $k_{nrad}$ ) (paths shown in Figure 13) are much smaller than the injection rate  $k_{inj}$ . The rate constant for charge injection  $k_{inj}$  is given by Fermi golden rule (Gratzel, 2001; Hara & Arakawa, 2003):

$$k_{inj} = \left( \frac{4\pi^2}{h} \right) |V|^2 \rho(E) \quad (11)$$

where  $h$  is Planck's constant,  $|V|$  is the electron-coupling matrix element and  $\rho(E)$  is the density of electronic acceptor states in the conduction band of the semiconductor. Equation (11) assumes that electron transfer from the excited dye molecules into the semiconductors is activationless and hence exhibits a temperature-independent rate. Some representative examples of electron injection rate constants  $k_{inj}$  and electronic coupling matrix elements  $|V|$  measured by laser flash photolysis for some sensitizers adsorbed onto nanocrystalline  $\text{TiO}_2$ ,  $t_f$  and  $\Phi_{inj}$  (the excited-state lifetime and the injection quantum yield, respectively) are presented in Table 4 (Gratzel, 2001; Hara & Arakawa, 2003). The shown values of  $|V|$  on Table 4 credited to the degree of overlapping of photosensitizer excited states wavefunction and the conduction band of the nanostructured photoelectrode. The distance between the adsorbed sensitizer and the nanostructured photoelectrode affect the value of the electronic coupling matrix elements.

Sensitizers	$k_{inj}$ [ $s^{-1}$ ]	$ V $ [ $cm^{-1}$ ]	$t_f$ [ns]	Quantum yield
$\text{Ru}^{II}(\text{bpy})_3$	$2 \times 10^5$	0.04	600	0.1
$\text{Ru}^{III}\text{L}_3 (\text{H}_2\text{O})$	$3 \times 10^7$	0.3	600	0.6
$\text{Ru}^{III}\text{L}_3 (\text{EtOH})$	$4 \times 10^{12}$	90	600	1.0
$\text{Ru}^{III}\text{L}_2(\text{NCS})_2$	$10^{13}$	130	50	1.0
Coumarin-343	$5 \times 10^{12}$	100	10	1.0
Eosin-Y	$9 \times 10^8$	2	1	0.4

Table 4. Electron injection rate constants  $k_{inj}$  and electronic coupling matrix elements  $|V|$  measured by laser flash photolysis for various sensitizers adsorbed onto nanocrystalline  $\text{TiO}_2$ . In the sensitizers column, L stands for the 4,4'-dicarboxy-2,2'-bipyridyl ligand and bpy for 2,2'-bipyridyl (From Gratzel, 2001).

Advantages of tandem structure have been investigated both theoretically and experimentally as approaches to improve the photocurrent of DSSC (Durr et al., 2004). "The

tandem structured cell exhibited higher photocurrent and conversion efficiency than each single DSSC mainly caused by its extended spectral response.” (Kubo et al., 2004)

### 3.3 Charge injection, transport, recombination, and cell dark current

Kinetics of electron injection into the semiconductor photoelectrode after being excited from the photosensitizer has been investigated by many researchers using time-resolved laser spectroscopy (Hara & Arakawa, 2003). It has been found that both the configuration of the photosensitizer material and the energy separation between the conduction band level of the wideband gap semiconductor and the LUMO level of the photosensitizer are greatly affecting the electron transfer rate to the wideband gap semiconductor. Figure 17 shows a schematic illustration of kinetics in the DSSC. The shown arrows indicate excitation of the dye from the HOMO to the LUMO level, relaxation of the excited state (60 ns), electron injection from the dye LUMO level to the TiO<sub>2</sub> conduction band (50 fs -1.7 ps), recombination of the injected electron with the hole in the dye HOMO level (ns -ms), recombination of the electron in the TiO<sub>2</sub> conduction band with a hole (I<sub>3</sub><sup>-</sup>) in the electrolyte (10 ms), and the regeneration of the oxidized dye by I<sup>-</sup> (10 ns). (Hagfeldt & Gratzel, 2000).

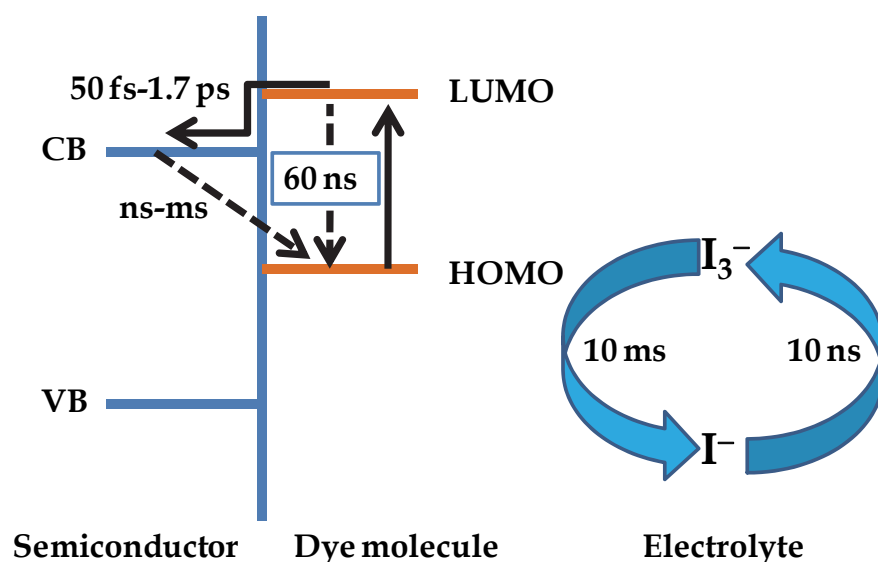


Fig. 17. Schematic illustration of kinetics in the DSSC, depicted from Hagfeldt & Gratzel, 2000.

It has been confirmed that electron injection from the excited dye such as the N<sub>3</sub> dye or RuL<sub>2</sub>(NCS)<sub>2</sub> complex into the TiO<sub>2</sub> conduction band (CB) is a very fast process in femtosecond scale. The reduction of the oxidized dye by the redox electrolyte's I<sup>-</sup> ions occur in about 10<sup>-8</sup> seconds. Recombination of photoinjected CB electrons with oxidized dye molecules or with the oxidized form of the electrolyte redox couple (I<sub>3</sub><sup>-</sup> ions) occurs in microseconds (Hara & Arakawa, 2003). To achieve good quantum yield, the rate constant for charge injection should be in the picosecond range. In conclusion, Fast recovery of the sensitizer is important for attaining long term stability. Also, long-lasting charge separation is a very important key factor to the performance of solar cells. Thus, new designs for larger conjugated dye-sensitizer molecules have been reported by investigators, for example, Haque et al., (Haque et al., 2004) studied hybrid supermolecules that are efficiently retard the recombination of the charge-separated state and therefore assure enhanced energy

conversion efficiency by extending the lifetime of light-induced charge-separated states as illustrated in Figure 18, “Hybrid supermolecule: This is the structure of the redox triad that gave the most efficient charge separation in the report by Haque and colleagues . The triad is made of a ruthenium complex anchored to nanocrystalline  $\text{TiO}_2$  (the electron acceptor) and covalently linked to polymeric chains of triphenyl-amine groups (the electron donor). Arrows represent the direction of the electron transfer process. The first step of the electron transfer is the light-induced excitation of the chromophore (process 1). Following this an electron is readily injected from the sensitizer excited state into the conduction band of the  $\text{TiO}_2$  semiconductor (process 2). The direct recombination of primarily separated charges (process 3) would degrade the absorbed energy into heat. In this supermolecule this is avoided through the fast reduction of the ruthenium by the linked triphenyl-amine electron donor groups (process 4). The secondary recombination process (process 5) between the injected electron and the oxidized amine radical is made increasingly slow because the positive charge can hop from one triphenylamine function to the adjacent one along the chain (process 6) and the hole moves away from the  $\text{TiO}_2$  surface. The overall photo-initiated process thus results in unidirectional electron flow from the end of the polymeric chains to the oxide (from right to left) and a very long-lived charge-separated state” (Moser, 2005).

In  $\text{TiO}_2$  nanoparticle DSSCs, the electrons diffuse to the anode by hopping 103-106 times between particles (Baxter et al., 2006). With each hop there is a considerable probability of recombination of the photoexcited electron with the electrolyte since both the diffusion and recombination rates are on the order of milliseconds. Hence, this allows recombination to limit the cell efficiency. On the other hand, nanowire or tube structured photoelectrode (e.g.,  $\text{ZnO}_2$ ) provide a direct path (express highway) to the anode, leading to increased diffusion rate without increasing the recombination rate and thus increases cell efficiency.

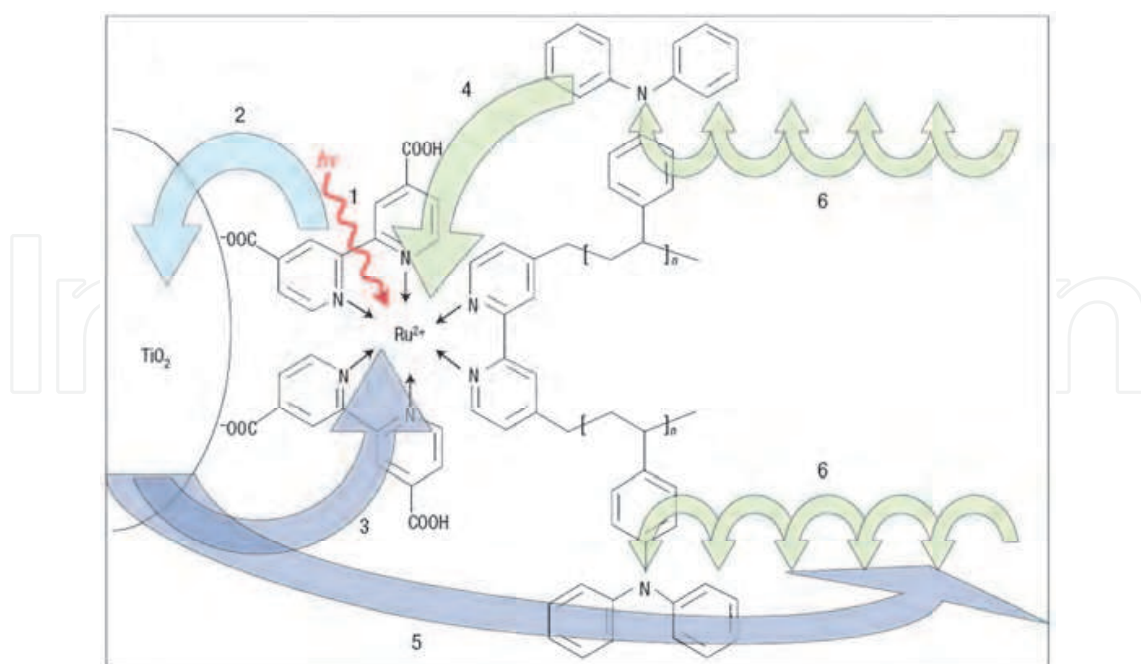


Fig. 18. Schematics of the hybrid supermolecule. The supersensitizer molecule adsorbed to a nanostructured  $\text{TiO}_2$  surface promise to improve the photovoltaic conversion efficiency of dye sensitized solar cell (From Moser, 2005).

Dark current in DSSC is mainly due to the loss of the injected electron from nanostructured wide bandgap semiconductor (say  $\text{TiO}_2$ ) to  $\text{I}_3^-$  (the hole carrier in solution electrolyte). Thus, it is a back reaction that must be eliminated or minimized. Reduction of dark current enhances the open circuit voltage of the cell, this can be deduced from the following general equation of solar cell relating the open circuit voltage  $V_{OC}$  to both the injection current  $I_{inj}$  and dark current  $I_{dark}$ :

$$V_{OC} = \frac{k_B T}{q} \ln \left( \frac{I_{inj}}{I_{dark}} + 1 \right) \quad (12)$$

where  $k_B$  is the Boltzmann constant,  $T$  is the absolute temperature of the cell, and  $q$  is the magnitude of the electron charge. In fact, dark current mainly occurs at the  $\text{TiO}_2$ /electrolyte interface where no photosensitizer got adsorbed. One successful way to suppress dark current is to use one of pyridine derivatives (e.g., tert-butylpyridine TBP) as coadsorbates on the nanostructured  $\text{TiO}_2$  surface. Figure 19 shows the current-voltage characteristics obtained for NKX-2311-sensitized  $\text{TiO}_2$  solar cells (Hara et al., 2003).

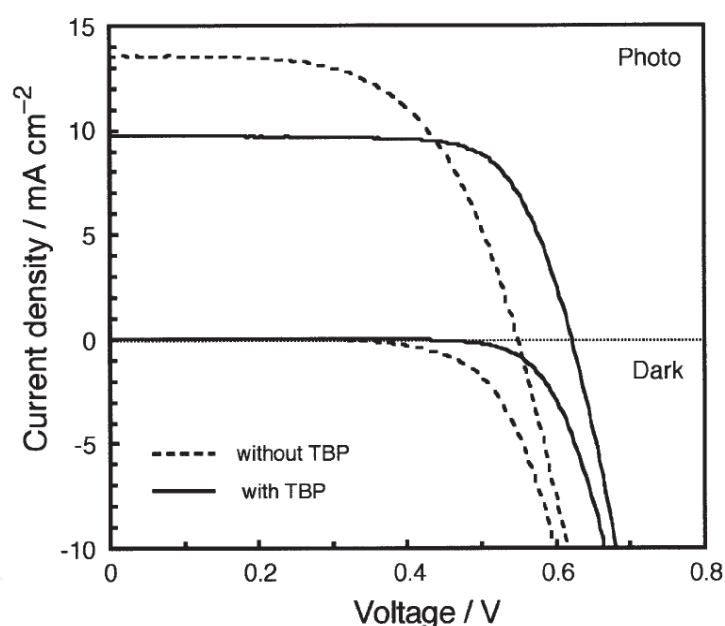


Fig. 19. Current-voltage curves obtained for NKX-2311-sensitized  $\text{TiO}_2$  solar cells in an electrolyte of 0.6M DMPImI-0.1M LiI-0.05M I<sub>2</sub> in methoxyacetonitrile: (---) without TBP, (—) with 0.5M TBP (From Hara et al., 2003).

#### 4. Applications of DSSC

Because of the physical nature of the dye sensitized solar cells, inexpensive, environment-friendly materials, processing, and realization of various colors (kind of the used sensitizing dye); power window and shingles are prospective applications in building integrated photovoltaics BIPV. The Australian company Sustainable Technologies International has produced electric-power-producing glass tiles on a large scale for field testing and the first building has been equipped with a wall of this type (see for example, Figure 20-a). The availability of lightweight flexible dye sensitized cells or modules are attractive for



applications in room or outdoor light powered calculators, gadgets, and mobiles. Dye sensitized solar cell can be designed as indoor colorful decorative elements (see Figure 20-b). Flexible dye sensitized solar modules opens opportunities for integrating them with many portable devices, baggage, gears, or outfits (Pagliaro et al., [www.pv-tech.org](http://www.pv-tech.org)) (see Figure 20-c and Figure 20-d). In power generation, dye sensitized modules with efficiency of 10% are attractive choice to replace the common crystalline Si-based modules. In 2010 Sony announced fabrication of modules with efficiency close to 10% and hence opportunity of commercialization of DSSC modules is attainable.

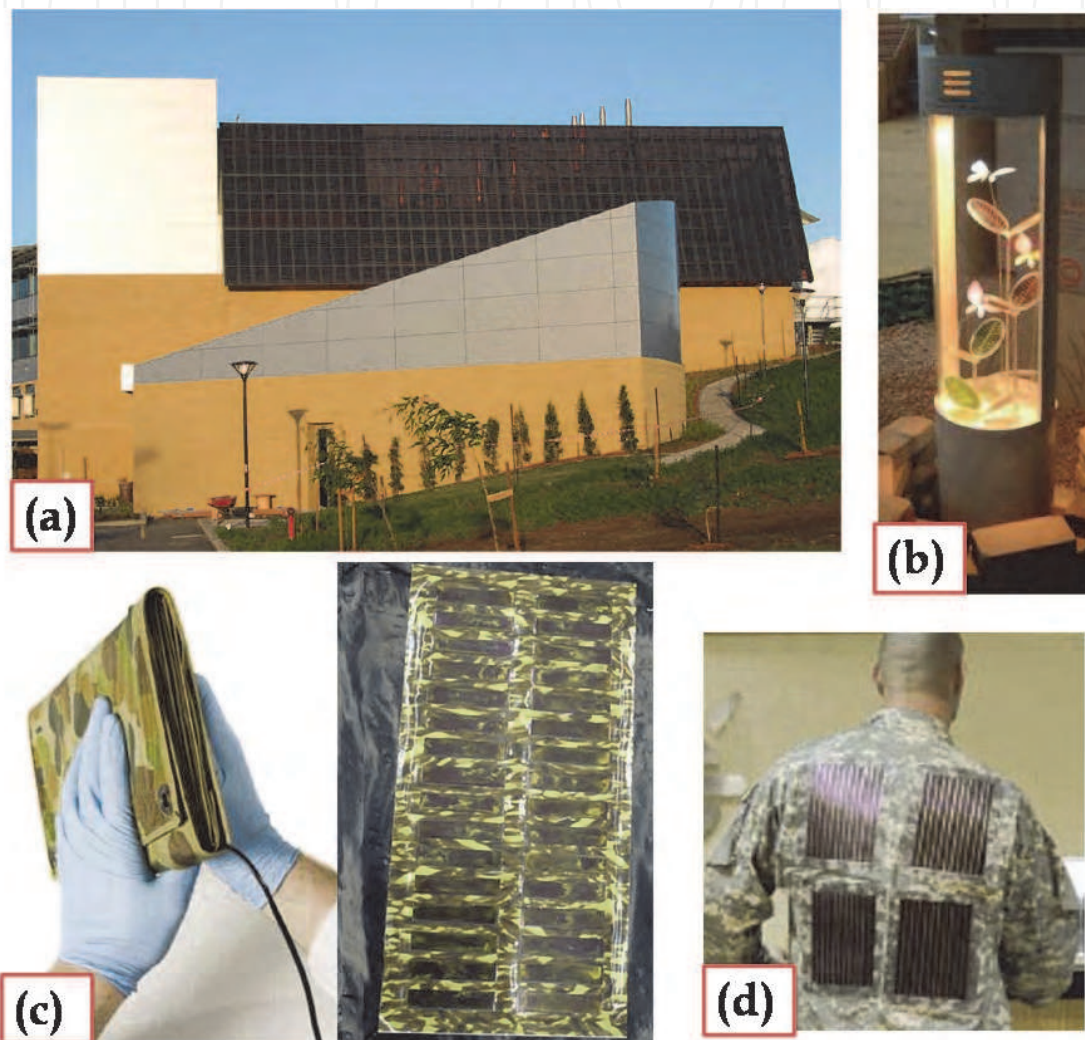


Fig. 20. Application examples of dye sensitized solar cells and modules: (a) 200 m<sup>2</sup> of STI DSSC panels installed in Newcastle (Australia)– the first commercial DSSC module (<http://www.sta.com.au/index.htm>), (b) indoor ornament of dye sensitized solar cells leaves (AISIN SEIKI CO.,LTD), (c) flexible DSSC-based solar module developed by Dyesol (<http://www.dyesol.com>), and (d) jacket commercialized by G24i (<http://www.g24i.com>).

## 5. Commercialization of DSSC

Commercialization of dye sensitized solar cells and modules is taking place on almost all continents (Lenzmann & Kroon, 2007). In Asia, specifically in Japan: IMRA-Aisin

Seiki/Toyota, Sharp, Toshiba, Dai Nippon, Peccell Technologies. In Australia: Dyesol. In USA Konarka. G24i in UK, and Solaronix in Switzerland. G24i has announced a DSC module production of 25MW capacity in 2007 in Cardiff, Wales (UK), with extension plans up to 200MW by the end of 2008 (<http://www.g24i.com>). The success of many labs and companies such as ASIAN and Toyota Central R & D Labs., INC. (see Figure 21) to demonstrate various sizes and colors in a series-connected dye solar cell module in many international exhibitions and conferences reflects the potential role of dye sensitized solar cells systems in the PV technology. In fact, Toyota has installed in their dream house walls a similar kind of DSSCs panels shown in Figure 21-b.

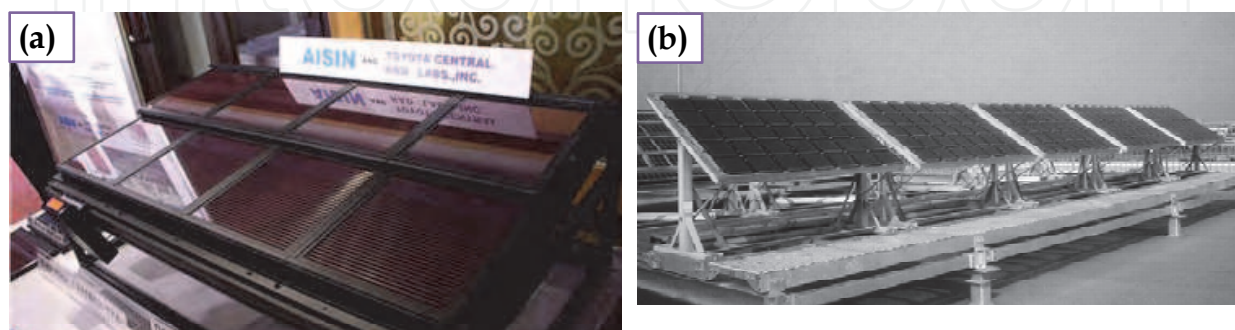


Fig. 21. (a) An example of DSSC module for outdoor application (From <http://kuroppe.tagen.tohoku.ac.jp/~dsc/cell.html>) and (b) Outdoor field tests of DSSC modules produced by Aisin Seiki in Kariya City. Note the pc-Si modules in the second row. (From Gratzel article at <http://rsta.royalsocietypublishing.org/content/365/1853/993.full#ref-3>).

Glass substrate is robust and sustains high temperatures, but it is fragile, nonflexible, and pricey when designed for windows or roofs. Flexible DSSCs have been intensively investigated. Miyasaka et. al. (Miyasaka & Kijitori, 2004) used the ITO (indium tin oxide) coated on PET (polyethylene terephthalate) as the substrate for DSSCs. Generally, the conducting glass is usually coated with nanocrystalline  $\text{TiO}_2$  and then sintered at  $450^\circ\text{C}$ - $500^\circ\text{C}$  to improve the electronic contact not only between the particles and support but also among the particles. Plastics films have a low ability to withstand heat. The efficiency of plastic-based dye sensitized solar cells is lower than that of using glass substrate ( $\eta = 4.1\%$ ,  $J_{sc} = 9.0\text{mA}/\text{cm}^2$ ,  $V_{oc} = 0.74\text{V}$ ,  $\text{FF} = 0.61$ ) because of poor necking of  $\text{TiO}_2$  particles. Kang et al., (Kang et al. 2006), used the stainless steel as the substrate for photoelectrode of DSSCs (see Figure 22). The cell illuminated through the counter electrode due to the non-penetration of light through metal substrate. In their system, the  $\text{SiO}_x$  layer was coated on stainless steel (sheet resistance  $\sim 1\text{ m}\Omega$  per square) and separated ITO from stainless steel, for preventing photocurrent leakage from stainless steel to the electrolyte. The constructed cells resulted in  $J_{sc} = 12\text{ mA}/\text{cm}^2$ ,  $V_{oc} = 0.61\text{ V}$ ,  $\text{FF} = 0.66$ , and  $\eta = 4.2\%$ . Recently, Chang et al. fabricated flexible substrate cell that produced conversion efficiency close to 2.91%. The photoelectrode substrates are flexible stainless steel sheet with thickness 0.07mm and titanium (Ti) sheet with thickness 0.25mm (Chang et al., 2010). Also, the reported approach by Yen et al. in developing a low temperature process for the flexible dye-sensitized solar cells using commercially available  $\text{TiO}_2$  nanoparticles (such as P25) is interesting since it yielded a conversion efficiency of 3.10% for an incident solar energy of  $100\text{ mW}/\text{cm}^2$  (Yen et al. 2010). Because Titanium has extremely high corrosion resistance, compared with stainless steel, Titanium is still the privileged substrate material.

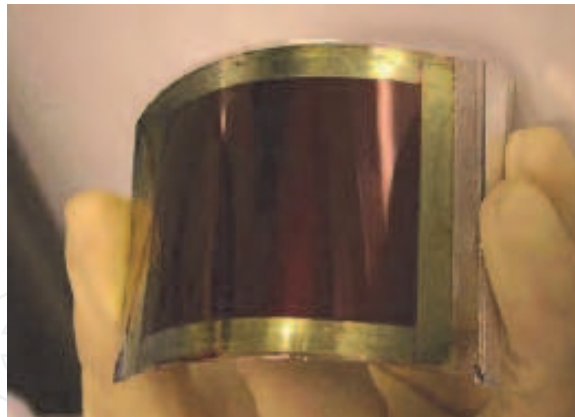


Fig. 22. A prototype of a flexible dye sensitized solar cell using stainless steel substrate (From Kang et al., 2006).

Availability of nonvolatile electrolyte is another issue toward commercialization of single or multi-junction modules. Polymer (solid) electrolyte, hole conductor, and solidified ionic liquids are solvent free choices with high electronic conductivity and chemical stability (Wang et al., 2005.) The key to high power heterojunction DSSC is to increase the effective diffusion length of electron within the nanostructured electrode by increasing the mobility of hole conductor or the extinction coefficient of the sensitizer to ensure more efficient light harvesting action. Since heat and UV light degrade cells performance, development of heat sink and optimized low cost UV coating is a must for outdoor applications. The successes in development of flexible substrate, solid electrolyte, and spectrally broad absorption range inexpensive nontoxic dyes will potentially open the possibility of role-to-role mass production of dye sensitized solar cells and modules (see Figure 23). Molecular engineering of efficient and stable organic sensitizers is an open invitation for many research groups, the successes in this area is expected to advance production and commercialization of DSSC (Kim et al., 2006).

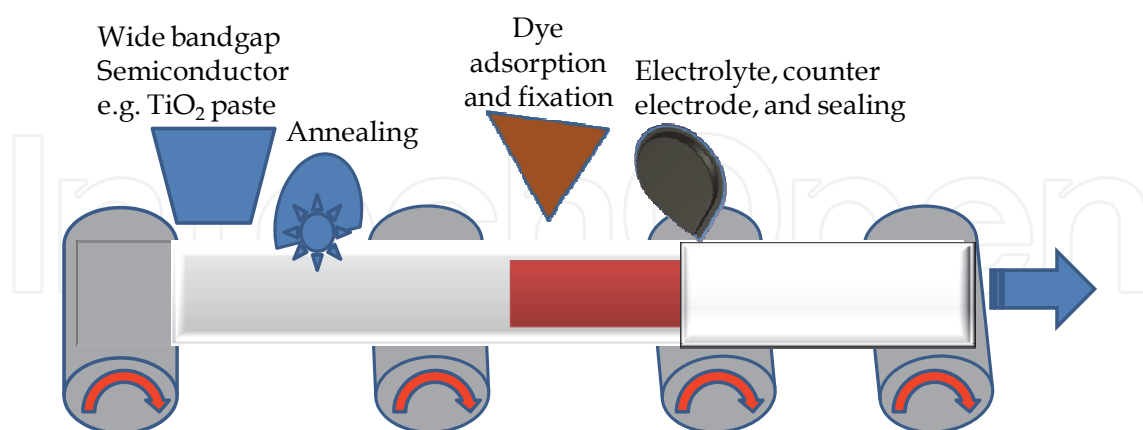


Fig. 23. Schematic of role-to-role manufacturing of flexible dye sensitized solar cells.

## 6. Conclusions

In This chapter we have discussed one example of the third generation solar cells, called photoelectrochemical cell and now called nanocrystalline dye sensitized solar cells DSSC or Gratzel cell. Nanocrystalline dye sensitized solar cell DSSC is classified as a low cost,

environmental friendly, and capable of being highly efficient cell mainly due to materials, charge carriers generation and transport within the cell structure. The nanostructured dye-sensitized solar cell (DSSC) is going to provide economically credible alternative to present day p-n junction photovoltaics. In fact, dye sensitized solar cell are green solar cell mimicking the green leaf. In dye sensitized solar cell electricity is generated as a result of electron transfer due to photoexcitation of dye molecules adsorbed to nanostructured wide bandgap material photoelectrode. The oxidized dye molecules regenerated by gaining electrons from electrolyte which is reduced by the electrons reaching the counter-electrode of the cell. In dye sensitized solar cells light absorption is separated from carrier transport. From educational point of view, since nanostructured dye sensitized solar cell DSSC is mimicking photosynthesis in plants, it provides an interdisciplinary context for students learning the basic principles of biological extraction, chemistry, physics, environmental science and electron transfer.

The requirements of practical sensitizers are: broad band and high level absorption of visible and near infrared region of the electromagnetic spectrum, exhibit thermal and photochemical stability, definitely chelating to the semiconductor oxide surface and inject electrons into the conduction band with a quantum yield of unity, and owning suitable ground- and excited state redox properties. Investigations of solvent free electrolyte such as polymer based, and ionic liquid are promising. In order to commercialize dye sensitized solar cell in low power applications, flexible DSSCs have been intensively investigated. The solar to electric power conversion efficiency of the DSC in full AM 1.5 sun light validated by accredited PV calibration laboratories has reached over 11 % and modules with efficiency close to 10% has been exhibited in 2010. Nanowires and quantum dots QDSSCs may be a promising solar cell design.

The search for green sources or generators of energy is considered one of the priorities in today's societies and occupies many policy makers' agendas. We at the University of Bahrain are the first to start the investigation of Dye sensitized solar cells DSSCs in the Arabian Gulf. Dye sensitized solar cells using natural organic dyes were prepared using low cost materials and natural dyes. Sensitization of wide gap oxides semiconductor materials was accomplished with the growth of nanocrystalline TiO<sub>2</sub>. The natural dyes extracted from Henna (*Lawsonia inermis* L.), pomegranate, cherries, and raspberries (*Rubus* spp.). We found that the nanocrystalline material based solar cell system exhibits an excellent optical absorption parameters for visible and near infrared portion of the electromagnetic spectrum. The performance of natural dye extract sensitized nanocrystalline solar cells can be appreciably enhanced by optimizing preparation technique, using different types of electrolyte, reported additives, and sealing.

In short, compared to Si based solar cells dye sensitized solar cells are of low cost and ease of production, their performance increases with temperature, possessing bifacial configuration - advantage for diffuse light, have transparency for power windows, color can be varied by selection of the dye, invisible PV-cells based on near-IR sensitizers are feasible, and they outperform amorphous Si. Moreover, DSSC shows higher conversion efficiency than polycrystalline Si in diffuse light or cloudy conditions. It is believed that nanocrystalline photovoltaic devices are becoming viable contender for large scale future solar energy converters.

## 7. Acknowledgments

The author is greatly indebted to the University of Bahrain for financial support. I would like to express my thanks to Prof. Dr. Shawqi Al Dallal for being keen in providing fruitful

discussions. Many thanks to Dr. Akil dakil (Department of Physics, University of Bahrain) for facilitating XRD measurements and Dr. Mohammad S. Hussain (National Nanotechnology Center King Abdulaziz City for Science and Technology (KACST)) for providing the SEM image.

## 8. References

- Amao, Y. & Komori, T. (2004). Bio-photovoltaic conversion device using chlorine- $e_6$  derived from chlorophyll from *Spirulina* adsorbed on a nanocrystalline  $TiO_2$  film electrode. *Biosensors Bioelectronics*, Vol. 19, Issue 8, pp. 843-847.
- Baxter, J.B; Walker, A.M; van Ommering, K. & Aydil, E.S. (2006). Synthesis and characterization of ZnO nanowires and their integration into dye-sensitized solar cells. *Nanotechnology*, Vol. 17, Issue 11, pp. S 304-S 312.
- Becquerel, A. E. (1839). Mmoire sur les effets électriques produits sous l'influence des rayons solaires. *C. R. Acad. Sci. Paris*, Vol. 9, pp. 561-567.
- Bergeron, B.V.; Marton, A.; Oskam, G. & Meyer, G.J. (2005). Dye-Sensitized  $SnO_2$  Electrodes with Iodide and Pseudohalide Redox Mediators. *J. Phys. Chem. B*, Vol, 109, pp.935-943.
- Boercker, J.E; Schmidt, J.B. & Aydil, E.S. (2009). Transport Limited Growth of Zinc Oxide Nanowires. *Cryst. Growth*, Vol. 9 (6), pp 2783-2789.
- Calogero, G.; Di Marco,G.; Caramori, S.; Cazzanti, S.; Roberto Argazzi, R. and Bignozzi, C.A. (2009). Natural dye sensitzers for photoelectrochemical cells. *Energy Environ. Sci.*, Vol. 2, Issue 11, pp. 1162-1172.
- Chang, H.; Chen, T.L.; Huang, K.D.; Chien, S.H. & Hung, K.C. (2010). Fabrication of highly efficient flexible dye-sensitized solar cells. *Journal of Alloys and Compounds*, Vol. 504, Issue 2, pp. S435-S438.
- Cherepy, N.J.; Smestad, G.P.; Gratzel, M. & Zhang, J.Z. (1997). Ultrafast Electron Injection: Implications for a Photoelectrochemical Cell Utilizing an Anthocyanin Dye-Sensitized  $TiO_2$  Nanocrystalline Electrode. *J. Phys. Chem. B*, Vol. 101, pp. 9342-9351.
- Chiba, Y.; Islam, A.; Watanabe, Y; Komiya, R.; Koide, N. & Han, L. (2006). Dye-sensitized solar cells with conversion efficiency of 11.1%. *Japanese Journal of Applied Physics, Part 2: Letters & Express Letters* , Vol. 45, pp. 24-28.
- Durr M.; Bamedi A.; Yasuda A. & Nelles G. (2004). Tandem dye-sensitized solar cell for improved power conversion efficiencies. *Appl. Phys. Lett.*, Volume 84 (17), pp. 3397-3399.
- Ellinson, R.; Beard, M.; Johnson, J.; Yu, P.; Micic, O.; Nozik, A.; Shabaev, A.; and Efros A. (2005). Highly Efficient Multiple Exciton Generation in Colloidal PbSe and PbS Quantum Dots, *Nano Letters*, Vol. 5, No. 5, pp. 865-871.
- Farzad, F.; Thompson, D. W.; Kelly, C. A.; and Meyer, G. J. (1999). Competitive Intermolecular Energy Transfer and Electron Injection at Sensitized Semiconductor Interfaces. *J. Am. Chem. Soc.*, Vol. 121, pp. 5577-5578.
- Fernando, J.M.R.C. & Senadeera G.K.R. (2008). Natural anthocyanins as photosensitizers for dye-sensitized solar devices. *Current Science*, Vol. 95, No. 5, pp. 663-666.
- Garcia, C.G., Polo, A.S. and Iha, N.Y. (2003). Fruit extracts and ruthenium polypyridinic dyes for sensitization of  $TiO_2$  in photoelectrochemical solar cells. *J. Photochem. Photobiol. A(Chem.)*, Vol. 160 (1-2), pp. 87-91.
- Gleiter, H. (1989). Nanocrystalline materials. *Prog. Mater. Sci.*, Vol. 33, pp. 223-315.

- Gratzel, M. & Hagfeldt, A. (2000). Molecular Photovoltaics. *Acc. Chem. Res*, Vol. 33, pp. 269-277.
- Gratzel, M. (2001). Molecular photovoltaics that mimic photosynthesis. *Pure Appl. Chem.*, Vol. 73, No. 3, pp. 459-467.
- Gratzel, M., (2003). Dye-sensitized solar cells. *Journal of Photochemistry and Photobiology C: Photochemistry Reviews* 4, pp. 145-153.
- Gratzel, M. (2005). Solar Energy Conversion by Dye-Sensitized Photovoltaic Cells. *Inorg. Chem.*, Vol. 44, pp. 6841-6851.
- Green, M. A.; Emery, K. Solar Cell Efficiency Tables 19, *Prog. Photovolt.: Res. Appl.* 2002; 10:55-61.
- Guo, M.; Diao, P.; Wang, X. & Cai, S. (2005). The effect of hydrothermal growth temperature on preparation and photoelectrochemical performance of ZnO nanorod array films. *Journal of Solid State Chemistry*, Vol., 178, pp. 3210-3215.
- Hao, S.; Wu, J.; Huang, Y. & Lin, J. (2006). Natural dyes as photosensitizers for dye-sensitized solar cell. *Sol. Energy*, Vol. 80, Issue 2, pp. 209-214.
- Hara, K. & Arakawa, H. (2003). Dye-sensitized Solar Cells, In: Handbook of Photovoltaic Science and Engineering, A. Luque and S. Hegedus, (Ed.), Chapter 15, pp. 663-700, John Wiley & Sons, Ltd, ISBN: 0-471-49196-9.
- Hara, K.; Tachibana, Y.; Ohgami, Y.; Shinohara, A.; Suganuma, S.; Sayama, K.; Sugihara, H. & Arakawa, H. (2003). Dye-sensitized nanocrystalline TiO<sub>2</sub> solar cells based on novel coumarin dyes. *Solar Energy Materials & Solar Cells*, Vol. 77, pp. 89-103.
- Haque, S.A.; Handa, A.; Katja, P.; Palomares, E.; Thelakkat, M. & Durrant, J.R. (2005). Supermolecular control of charge transfer in dye-sensitized nanocrystalline TiO<sub>2</sub> films: towards a quantitative structure-function relationship. *Angewandte Chemie International Edition*, Vol. 44, pp. 5740-5744.
- Harding, H.E.; Hoke, E.T.; Armstrong, P.B.; Yum, J.; Comte, P.; Torres, T.; Frechet, J.M.J.; Nazeeruddin, M.K.; Gratzel, M. & McGehee, M.D. (2009). Increased light harvesting in dye-sensitized solar cells with energy relay dyes. *Nature Photonics*, Vol. 3, pp. 406-411.
- Hasobe, T.; Fukuzumi, S. & Kamat, P.V. (2006). Organized Assemblies of Single Wall Carbon Nanotubes and Porphyrin for Photochemical Solar Cells: Charge Injection from Excited Porphyrin into Single-Walled Carbon Nanotubes. *Journal of Physical Chemistry B*, Vol. 110 (50), pp. 25477-25484.
- Hasselmann, G. & Meyer, G. (1999). Sensitization of Nanocrystalline TiO<sub>2</sub> by Re(I) Polypyridyl Compounds. *J. Phys. Chem.*, Vol. 212, pp. 39-44.
- Hirata, N.; Lagref, J.; Palomares, E.J.; Durrant, J.R.; M. Khaja Nazeeruddin, Gratzel, M. & Di Censo, D. (2004). Supramolecular Control of Charge-Transfer Dynamics on Dye-sensitized Nanocrystalline TiO<sub>2</sub> Films. *Chem. Eur. J.* Vol. 10, Issue 3, pp. 595-602.
- Hoffert, M.I.; Caldeira, K.; Jain, A.K.; Haites, E.F.; Harvey, L.D.; Potter, S.D.; Schlesinger, M.E.; Schneider, S.H.; Watts, R.G.; Wigley, T.M. & Wuebbles, D.J. (1998). Energy implications of future stabilization of atmospheric CO<sub>2</sub> content. *Nature*, Vol. 395, pp. 881-884.
- Horiuchi, T.; Hidetoshi Miura, H.; Sumioka, K. & Satoshi Uchida, S. (2004). High Efficiency of Dye-Sensitized Solar Cells Based on Metal-Free Indoline Dyes. *J. Am. Chem. Soc.*, Vol. 126 (39), pp 12218-12219.

- Hoyer, P. & Könenkamp, R., (1995). Photoconduction in porous TiO<sub>2</sub> sensitized by PbS quantum dots. *Appl. Phys. Lett.* Vol. 66, Issue 3, pp. 349-351.
- Islam, A.; Hara, K.; Singh, L. P.; Katoh, R.; Yanagida, M.; Murata, S.; Takahashi, Y.; Sugihara, H. & Arakawa, H. (2000) *Chem. Lett.*, pp. 490-491.
- Jasim, K. E. & Hassan, A.M. (2009). Nanocrystalline TiO<sub>2</sub> based natural dye sensitised solar cells. *Int. J. Nanomanufacturing*, Vol. 4, Nos. 1/2/3/4, pp.242-247.
- Jasim, K. E.; Al Dallal, S. & Hassan, A.M. (2011). Natural dye-sensitized photovoltaic cell based on nanoporous TiO<sub>2</sub>, *Int. J. Nanoparticles*, (in press 2011).
- Jasim, K. E.; Al Dallal, S. & Hassan, A.M. (2011). HENNA (*Lawsonia inermis* L.) DYE-SENSITIZED NANOCRYSTALLINE TITANIA SOLAR CELL. *J. Nanotechnology*, submitted for publication.
- Jasim, K. E. (2011). Natural Dye-Sensitized Solar Cell Based On Nanocrystalline TiO<sub>2</sub>. *Sains Malaysiana*, submitted for publication.
- En Mei Jin; Kyung-Hee Park; Bo Jin; Je-Jung Yun, & Hal-Bon Gu (2010). Photosensitization of nanoporous TiO<sub>2</sub> films with natural dye. *Phys. Scr.* Vol. 2010, Issue T139, pp. 014006.
- Jiu, J., Wang, F., Isoda, S., and Adachi, M. (2006). *J Phys Chem B Condens Matter Mater Surf Interfaces Biophys.*, Vol. 110(5), pp. 2087-2092
- Kang, M.G., Park, N-G., Kim, K-M., Ryu, K.S., Chang S.H. & Kim, K.J. (2003). Highly efficient polymer gel electrolytes for dye-sensitized solar cells. *3rd World Conference on Photovoltaic Energy Conversion*. May 11-18, 2003 Osh, Japan.
- Kang, M.; Park, N.; Ryu, K.; Chang, S. & Kim, K. (2006). A 4.2% efficient flexible dye-sensitized TiO<sub>2</sub> solar cells using stainless steel substrate. *Solar Energy Materials & Solar cells*, Vol. 90, pp. 574-581.
- Karami, A. (2010). Synthesis of TiO<sub>2</sub> Nano Powder by the Sol-Gel Method and Its Use as a Photocatalyst. *J. Iran. Chem. Soc.*, Vol. 7, pp. S154-S160.
- Kawano, R.; Matsui, H.; Matsuyama, C.; Sato, A.; Susan, Md. A. B.H.; Tanabe, A. & Watanabe, M. (2004). High performance dye-sensitized solar cells using ionic liquids as their electrolytes. *Journal of Photochemistry and Photobiology A*, Vol. 164, no. 1-3, pp. 87-92.
- Kelly, C. A.; Thompson, D. W.; Farzad, F. & Meyer, G. J. (1999). Excited State Deactivation of Ruthenium(II) Polypyridyl Chromophores Bound to Nanocrystalline TiO<sub>2</sub> Mesoporous Films. *Langmuir*, Vol. 15, pp. 731-734.
- Kim, K.S.; Kang, Y.S.; Lee, J.H.; Shin, Y.J.; Park, N.G.; Ryu, K.S. & Chang, S.H. (2006). Photovoltaic properties of nano-particulate and nanorod array ZnO electrodes for dye-sensitized solar cell. *Bull Korean Chem. Soc*, Vol. 27, pp. 295-298.
- Kim, S.; Lee, J.K.; Kang, S.O.; Ko, J.J.; Yum, J.H.; Fantacci, S.; De Angelis, F.; Di Censo, D.; Nazeeruddin, Md. K. & Graetzel, M., (2006). Molecular Engineering of Organic Sensitizers for Solar Cell Applications. *J. Am. Chem. Soc*, Vol. 128, pp. 16701-16707.
- Kleverlaan, C. J.; Indelli, M. T.; Bignozzi, C. A.; Pavanin, L.; Scandola, F. & Hasselmann, Meyer, G. J. (2000). Stepwise Photoinduced Charge Separation in Heterotriads: Binuclear Rh(III) Complexes on Nanocrystalline Titanium Dioxide. *J. Am. Chem. Soc.*, Vol. 122, pp. 2840-2849.
- Kopidakis, N.; Benkstein, K.D.; van de Lagemaat, J. & Frank, A.J. (2003). *J. Phys. Chem. B*, Vol. 107, pp. 11307.

- Kuang, D.; Wang, P.; Ito, S.; Zakeeruddin, S.M. & Gratzel, M. (2006). Stable mesoscopic dye-sensitized solar cells based on tetracyanoborate ionic liquid electrolyte. *Journal of the American Chemical Society*, Vol. 128, no. 24, pp. 7732-7733.
- Kubo, W.; Murakoshi, K.; Kitamura, T.; Yoshida, S.; Haruki, M.; Hanabusa, K.; Shirai, H.; Wada, Y., & Yanagida, S. (2001). Quasi-Solid-State Dye-Sensitized TiO<sub>2</sub> Solar Cells: Effective Charge Transport in Mesoporous Space Filled with Gel Ele, . *J Phys. Chem. B*, Vol. 105, Issue 51, pp. 12809-12812.
- Kubo, W.; Sakamoto, A.; Kitamura, T.; Wada, Y. & Yanagida, S. (2004). Dye-sensitized solar cells: improvement of spectral response by tandem structure, *Journal of Photochemistry and Photobiology A: Chemistry*, Vol.164, pp. 33-39.
- Kumara, G.R.A., Kanebo, S., Okuya, M., Onwaona-Agyeman, B., Konno, A., and Tennakone, K. (2006) . *Sol. Enrgy Mater. Sol. Cells*, Vol. 90, pp.1220.
- Lagref, J.J.; Nazeeruddin, M.K., & Graetzel, M. (2008). Artificial photosynthesis based on dye-sensitized nanocrystalline TiO<sub>2</sub> solar cells, *INORGANICA CHIMICA ACTA*, Vol. 361, Issue 3, pp.735-745.
- Law, M.; Greene, L. E.; Johnson, J. C.; Saykally, R. & Yang, P. D. (2005). Nanowire dye-sensitized solar cells. *Nature Materials*, Vol. 4, 455-459.
- Lenzmann, F.O. & Kroon, J.M. (2007). Recent Advances in Dye-Sensitized Solar Cells, *Advances in OptoElectronics* , Volume 2007, Article ID 65073.
- Lewis, N. S. (2007). Toward Cost-Effective Solar Energy Use. *Science*, Vol 315, pp. 798-801.
- Lindström, H.; Holmberg, A.; Magnusson, E.; Malmqvist, L. & Hagfeldt, A. (2001). A new method to make dye-sensitized nanocrystalline solar cells at room temperature, *Journal of Photochemistry and Photobiology A: Chemistry*, Vol. 145, pp. 107-112.
- Liu, D. and Kamat, P.V. (1993). Photoelectrochemical behavior of thin cadmium selenide and coupled titania/cadmium selenide semiconductor films. *J. Phys. Chem.* Vol. 97, pp. 10769-10773.
- Martinson, A. B. F.; Hamann, T. W.; Pellin, M. J. & Hupp, J. T. (2008). New Architectures for Dye-Sensitized Solar Cells. *Chem. – Eur. J.*, Vol. 14, 4458- 4467.
- Matsumoto, M.; Wada, Y.; T. Kitamura, T.; Shigaki, K.; Inoue, T.; Ikeda, M. and Yanagida, S. (2001). Fabrication of solid-state dye-sensitized TiO<sub>2</sub> solar cell using polymer electrolyte. *Bull. Chem. Soc. Japan*, vol. 74, pp. 387-393.
- Miyasaka, T. & Kijitori, Y. (2004). Low-temperature fabrication of dye-sensitized plastic electrodes by electrophoretic preparation of mesoporous TiO<sub>2</sub> layers. *J. Electrochem. Soc.*, Vol. 151(11), pp. A1767-A1773.
- Monari, A.; Assfeld, X.; Beley, M. & Gros, P.C. (2011). Theoretical Study of New Ruthenium-Based Dyes for Dye-Sensitized Solar Cells. *J. Phys. Chem. A*, Vol.115 (15), pp. 3596-3603.
- Mor, G.K.; Shankar, K.; Paulose, M.; Varghese, O.K. & Grimes, C.A. (2006). Use of Highly-Ordered TiO<sub>2</sub> Nanotube Arrays in Dye-Sensitized Solar Cells. *Nanoletters*, Vol., 6, Issue 2, p.215-218.
- Moser, J.-E. (2005). Solar Cells Later rather than sooner, *Nature materials*, Vol. 4, pp. 723-724.
- Nansen, R. (1995). *Sun Power: The Global Solution for the Coming Energy Crisis*. Ocean Press, ISBN-10: 0964702118, Washington, USA.
- Nazerruddin, M.K; Kay, A.; Ridicio, I.; Humphry-Baker, R.; Mueller, E.; Liska, P.; Vlachopoulos, N. & Gratzel, M. (1993). *J. Amer. Chem. Soc.* Vol. 115, pp. 6382-6390.



- Nazeeruddin, M. K.; De Angelis, F.; Fantacci, S.; Selloni, A.; Viscardi, G.; Liska, P.; Ito, S.; Takeru, B., & Graetzel, M. (2005). Combined Experimental and DFT-TDDFT Computational Study of Photoelectrochemical Cell Ruthenium Sensitizers. *J. Am. Chem. Soc.*, Vol. 127(48), pp. 16835-16847.
- Noack, V., Weller, H., & Eychmuller, A. (2002). *J. Phys. Chem. B*, Vol. 106, pp. 8514.
- Nogueira, A.F.; De Paoli, M.A.; Montanan, I.; Monkhouse, R. & Durrant, I. (2001). *J. Phys. Chem. B*, Vol. 105, pp. 7417.
- Nozik, A.J. (2001). Quantum Dot Solar Cells. *Annu. Rev. Phys. Chem.* Vol. 52, pp. 193-231.
- Nozik, A. J. (2004). Quantum dot solar cells. *Next Gener. Photovoltaics*, pp. 196-222.
- Nozik, A. J. (2005). Exciton multiplication and relaxation dynamics in quantum dots: applications to ultrahigh-efficiency solar photon conversion. *Inorg. Chem.* Vol. 44, pp. 6893-6899.
- O'Regan B. & Gratzel, M. (1991). A low cost, high-efficiency solar cell based on dye-sensitized colloidal TiO<sub>2</sub> films. *Nature*; Vol. 353, pp. 737-739.
- Pagliaro, M.; Palmisano, G., & Ciriminna, R. (2008). Working principles of dye-sensitized solar cells and future applications, third print edition of *Photovoltaics International journal*, www.pv-tech.org.
- Pavasupree, S.; Suzuki, Y.; Yoshikawa, S., & Kawahata, R. (2005). Synthesis of Titanate, TiO<sub>2</sub>(B), and Anatase TiO<sub>2</sub> Nanofibers from Natural Rutile Sand, *J. Solid State Chem.*, Vol. 178 (10), pp. 3110-3116.
- Pavasupree, S.; Ngamsinlapasathian, S.; Nakajima, M.; Suzuki, Y., & Yoshikawa, S. (2006). Synthesis, characterization, photocatalytic activity and dye-sensitized solar cell performance of nanorods/nanoparticles TiO<sub>2</sub> with mesoporous structure, *Journal of Photochemistry and Photobiology A: Chemistry*, Vol. 184. pp 163-169.
- Plass, R.; Pelet, S.; Krueger, J., & Gratzel, M. (2002). Quantum Dot Sensitization of Organic-Inorganic Hybrid Solar Cells, *Phys. Chem. B*, Vol. 106 (31), pp. 7578-7580.
- Polo, A.S., and Iha, N.Y. (2006). Blue sensitizers for solar cells: natural dyes from Calafate and Jaboticaba. *Sol. Energy Mater. Sol. Cells*, Vol. 90, pp.1936-1944.
- Qu, P.; Thompson, D. W., & Meyer, G. J. (2000). Temperature Dependent, Interfacial Electron Transfer from Ru(II) Polypyridyl Compounds with Low Lying Ligand Field States to Nanocrystalline Titanium Dioxide. *Langmuir*, Vol. 16, pp. 4662-4671.
- Ren, Y.; Zhang, Z.; Gao, E.; Fang, S., & Cai, S. (2001). A dye-sensitized nanoporous TiO<sub>2</sub> photoelectrochemical cell with novel gel network polymer electrolyte. *J. Appl. Electrochem.*, Vol. 31, pp. 445-447.
- Robel, I.; Bunker, B. A. & Kamat, P. V. (2005). Single-walled carbon nanotube-CdS nanocomposites as light-harvesting assemblies: Photoinduced charge-transfer interactions, *Adv. Mater.*, 17, 20, pp. 2458-2463.
- Sayer, R. A.; Hodson, S.L. & Fisher, T.S. (2010). Improved Efficiency of Dye-Sensitized Solar Cells Using a Vertically Aligned Carbon Nanotube Counter Electrode, *J. Sol. Energy Eng.*, Vol. 132, Issue 2, 021007 (4 pages).
- Schmidt-Mende, L. & Gratzel, M. (2006). TiO<sub>2</sub> pore-filling and its effect on the efficiency of solid-state dye-sensitized solar cells, *Thin Solid Films* 500, pp. 296-301.
- Shen, Q., Katayama, K., Sawada, T., Yamaguchi, M., and Toyoda, T. (2006). Optical Absorption, Photoelectrochemical, and Ultrafast Carrier Dynamic Investigations of TiO<sub>2</sub> Electrodes Composed of Nanotubes and Nanowires Sensitized with CdSe Quantum Dots, *Japanese Journal of Applied Physics*, Vol. 45, No. 6B, pp. 5569-5574.

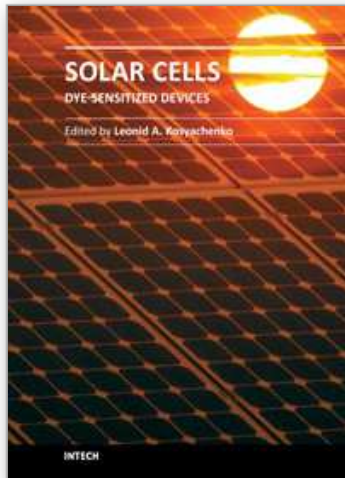
- Shoute, L. C. T., & Loppnow, G. R. (2003). Excited-state Metal-to-Ligand Charge Transfer Dynamics of a Ruthenium(II) Dye in Solution and Adsorbed on TiO<sub>2</sub> Nanoparticles from Resonance Raman Spectroscopy. *J. Am. Chem. Soc.*, Vol.125, pp.15636-15646.
- Smestad, G.P. (1998). Education and solar conversion: Demonstrating electron transfer, *Sol. Energy Mater. Sol. Cells*, Vol. 55, pp. 157-178.
- Smestad, G.P. & Gratzel, M. (1998). Demonstrating Electron Transfer and Nanotechnology: A Natural Dye-Sensitized Nanocrystalline Energy Converter, *Journal of Chemical Education*, Vol. 75 No. 6, pp. 752-756.
- Späth, M., Sommeling, P. M., van Roosmalen, J. A. M., Smit, H. J. P., van der Burg, N. P. G., Mahieu, D. R., Bakker, N. J. & Kroon, J. M. (2003). Reproducible Manufacturing of Dye-Sensitized Solar Cells on a Semi-automated Baseline, *Prog. Photovolt: Res. Appl.* Vol. 11, pp. 207-220.
- Suri, P., Panwar, M., & Mehra, R. (2007). Photovoltaic performance of dye-sensitized ZnO solar cell based on Eosin-Y photosensitizer, *Materials Science-Poland*, Vol. 25, No. 1, pp. 137-144.
- SSun, J.Q.; Wang, J.S.; Wu, X.C.; Zhang, G.S.; Wei, J.Y.; Zhang, S.Q.; Li, H. & Chen, D.R. (2006). Novel Method for High-Yield Synthesis of Rutile SnO<sub>2</sub> Nanorods by Oriented Aggregation. *Crystal Growth & Design*, Vol., 6, Issue 7, pp.1584-1587.
- Suzuki, Y.; Ngamsinlapasathian, S.; Yoshida, R., & Yoshikawa, S. (2006). Partially nanowires-structured porous TiO<sub>2</sub> electrode for dye-sensitized solar cell. *Central Euro. J. Chem.*, Vol. 4 (3), pp. 476 -488.
- Tennakone, K.; Kumara, G.; Kottegoda, I. & Wijayantha, K. (1997). The photostability of dye-sensitized solid state photovoltaic cells: factors determining the stability of the pigment in n-TiO<sub>2</sub>/Cyanidin/p-CuI cells. *Semicond. Sci. Technol.* Vol. 12, pp. 128.
- Tennakone, K.; Perera, V.P.S; Kottegoda, I.R.M. & Kumara, G. (1999). Dye-sensitized solid state photovoltaic cell based on composite zinc oxide/tin (IV) oxide films, *J. Phys. D-App. Phys.*, Vol. 32, No. 4, pp. 372.
- Tiwari, A., & Snure, M. (2008). Synthesis and Characterization of ZnO Nano-Plant-Like Electrodes. *Journal of Nanoscience and Nanotechnology*, Vol. 8, pp. 3981-3987.
- Vogel, R. & Weller. H. (1994). Quantum-Sized PbS, CdS, Ag<sub>2</sub>S, Sb<sub>2</sub>S<sub>3</sub>, and Bi<sub>2</sub>S<sub>3</sub> Particles as Sensitizers for Various Nanoporous Wide- Bandgap Semiconductors. *J. Phys. Chem.* Vol. 98, pp. 3183-3188.
- Wang, P., Zakeeruddin, S.M., Moser, J.-E., Humphry-Baker, R., and Gratzel, M. (2004). "A solvent-free, SeCN<sup>-</sup>/(SeCN)<sub>3</sub><sup>-</sup> based ionic liquid electrolyte for high-efficiency dye-sensitized nanocrystalline solar cells," *Journal of the American Chemical Society*, vol. 126, no. 23, pp. 7164-7165.
- Wang, P.; Klein, C.; Humphry-Baker, R.; Zakeeruddin, S. M. & Gratzel, M. (2005). Stable >= 8% efficient nanocrystalline dye-sensitized solar cell based on an electrolyte of low volatility. *Appl. Phys. Lett.* Vol. 86 (12), pp. Art. No.123508.
- Wongcharee, K.; Meeyoo, V. & Chavadej, S. (2007). Dye-sensitized Solar Cell Using Natural Dye Extract From Rosslea and Blue Pea Flower . *Sol. Enrgy. Mater. Sol. Cells*, Vol. 91 (7), pp. 566-571.

www.g24i.com

www.intertechpira.com

- Xiang, J.H., Zhu, P.X., Masuda, Y., Okuya, M., Kaneko, S. & Koumoto, K. (2006). Flexible solar-cell from zinc oxide nanocrystalline sheets self-assembled by an in-situ electrodeposition process. *J. Nanosci. Nanotechnol.* Vol. 6 (6), pp. 1797-1801.
- Yanagida, S., (2006). Recent research progress of dye-sensitized solar cells in Japan. *C. R. Chimie.* Vol. 9, pp. 597-604.
- Yang, M., Thompson, D., and Meyer, G. (2000). Dual Sensitization Pathways of TiO<sub>2</sub> by Na<sub>2</sub>[Fe(bpy)(CN)<sub>4</sub>]. *Inorg. Chem.* Vol. 39, pp. 3738-3739.
- Yanagida, S., Senadeera, G.K.R., Nakamura, K., Kitamura, T., & Wada, Y. (2004). Polythiophene-sensitized TiO<sub>2</sub> solar cells. *J. Photochem. Photobiol. A*, Vol. 166, pp. 75-80.
- Yen, W.; Hsieh, C.; Hung, C.; Hong-Wen Wang, H., & Tsui, M. (2010). Flexible TiO<sub>2</sub> Working Electrode for Dye-sensitized Solar Cells. *Journal of the Chinese Chemical Society*, Vol 57, pp.1162-1166.
- Zaban, A.; Micic, O.I.; Gregg, B.A. & Nozik, A.J. (1998). Photosensitization of Nanoporous TiO<sub>2</sub> Electrodes with InP Quantum Dots. *Langmuir*, Vol. 14 (12), pp. 3153-3156.
- Zhang, W.; Zhu, R.; Li, F.; Qing Wang, Q. & Bin Liu, B. (2011). High-Performance Solid-State Organic Dye Sensitized Solar Cells with P3HT as Hole Transporter. *J. Phys. Chem. C*, Vol. 115 (14), pp 7038-7043.
- Zhu, K.; Neale, N.R.; Halverson, A.F.; Kim, J.Y. & Frank, A.J. (2010). Effects of Annealing Temperature on the Charge-Collection and Light-Harvesting Properties of TiO<sub>2</sub> Nanotube-Based Dye-Sensitized Solar Cells. *J. Phys. Chem. C*, Vol. 114 (32), pp 13433-13441.
- Zhao, J.; Wang, A. & Green, M.A. (1999). 24.5% Efficiency Silicon PERT Cells on MCZ Substrates and 24.7% Efficiency PERL Cells on FZ Substrates. *Progress in Photovoltaics*, Vol. 7, pp. 471-474.
- Zweibel, K. & Green, M.A. (ed.) (2000). *Progress in Photovoltaics: Research and Applications*, Volume 8, Issue 1, pp. 171 - 185, John Wiley & Sons, Ltd;

IntechOpen



## **Solar Cells - Dye-Sensitized Devices**

Edited by Prof. Leonid A. Kosyachenko

ISBN 978-953-307-735-2

Hard cover, 492 pages

**Publisher** InTech

**Published online** 09, November, 2011

**Published in print edition** November, 2011

The second book of the four-volume edition of "Solar cells" is devoted to dye-sensitized solar cells (DSSCs), which are considered to be extremely promising because they are made of low-cost materials with simple inexpensive manufacturing procedures and can be engineered into flexible sheets. DSSCs are emerged as a truly new class of energy conversion devices, which are representatives of the third generation solar technology. Mechanism of conversion of solar energy into electricity in these devices is quite peculiar. The achieved energy conversion efficiency in DSSCs is low, however, it has improved quickly in the last years. It is believed that DSSCs are still at the start of their development stage and will take a worthy place in the large-scale production for the future.

### **How to reference**

In order to correctly reference this scholarly work, feel free to copy and paste the following:

Khalil Ebrahim Jasim (2011). Dye Sensitized Solar Cells - Working Principles, Challenges and Opportunities, Solar Cells - Dye-Sensitized Devices, Prof. Leonid A. Kosyachenko (Ed.), ISBN: 978-953-307-735-2, InTech, Available from: <http://www.intechopen.com/books/solar-cells-dye-sensitized-devices/dye-sensitized-solar-cells-working-principles-challenges-and-opportunities>

**INTECH**  
open science | open minds

### **InTech Europe**

University Campus STeP Ri  
Slavka Krautzeka 83/A  
51000 Rijeka, Croatia  
Phone: +385 (51) 770 447  
Fax: +385 (51) 686 166  
[www.intechopen.com](http://www.intechopen.com)

### **InTech China**

Unit 405, Office Block, Hotel Equatorial Shanghai  
No.65, Yan An Road (West), Shanghai, 200040, China  
中国上海市延安西路65号上海国际贵都大饭店办公楼405单元  
Phone: +86-21-62489820  
Fax: +86-21-62489821

© 2011 The Author(s). Licensee IntechOpen. This is an open access article distributed under the terms of the [Creative Commons Attribution 3.0 License](#), which permits unrestricted use, distribution, and reproduction in any medium, provided the original work is properly cited.

IntechOpen

IntechOpen